Durability of Polymer Electrolyte Membrane Fuel Cell (PEMFC) Directly Hybridized with Supercapacitor Storage Devices

A Major Qualifying Project Report

Submitted to the faculty

Of the

Worcester Polytechnic Institute

In partial fulfillment of the requirements for the

Degree of Bachelor of Science

By

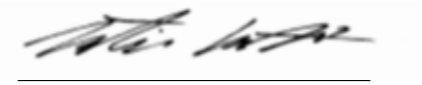

Martin Burkardt

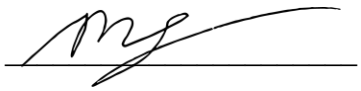

Marcus Lundgren

This report represents work of WPI undergraduate students submitted to the faculty as evidence of a degree requirement. WPI routinely publishes these reports on its web site without editorial or peer review. For more information about the projects program at WPI, see http://www.wpi.edu/Academics/Projects.

Abstract

Fuel cells (FC), modular energy conversion devices, convert the chemical energy of an appropriate fuel directly to electrical energy efficiently and with low emissions; gaining the interest of many industries as a potential energy source that can reduce environmental impact and geopolitical consequences compared to other fuel sources. Among other FCs, polymer electrolyte membrane fuel cells (PEMFC) are particularly popular because of their high energy density, compact size and ease of operation. PEMFCs are also leading in commercialization of FC technology, nevertheless, further research and development are required and it is imperative to understand the principles of FC operation in combination with an outlook to overcome obstacles related to the technology such as high capital investment costs, manufacturing costs and degradation of the FC materials.

We investigated the behavior of PEMFCs in cyclic operation, simulating use in transportation applications, and the aging process. This was done by requesting a range of current loads from the cell; representing typical automotive conditions transitioning through abrupt acceleration, deceleration, traffic stagnancy, and highway operation. This study aims to compare non-hybridized (without supercapacitor (SC)) FC degradation and durability with previously studied hybridized configurations, all run with the same stoichiometric and I_{SL} (current safety limit) conditions.

Résumé

Les piles à combustible (FC), des dispositifs de conversion d'énergie modulaires, convertissent l'énergie chimique d'un combustible approprié directement en énergie électrique efficacement et avec de faibles émissions; susciter l'intérêt de nombreuses industries en tant que source d'énergie potentielle pouvant réduire l'impact environnemental et les conséquences géopolitiques par rapport aux autres sources d'énergie. Parmi les autres FC, les piles à combustible à membrane électrolyte polymère (PEMFC) sont particulièrement populaires en raison de leur densité énergétique élevée, de leur taille compacte et de leur facilité d'utilisation. Les PEMFC sont également leaders dans la commercialisation de la technologie FC, mais d'autres recherches et développements sont nécessaires et il est impératif de comprendre les principes de fonctionnement de FC en conjonction avec une perspective pour surmonter les obstacles liés à la technologie tels que coûts d'investissement élevés, coûts de fabrication et la dégradation des matériaux FC.

Nous étudions actuellement le comportement des PEMFC en fonctionnement cyclique, en simulant l'utilisation dans les applications de transport et le processus de vieillissement. Ceci est fait en demandant une gamme de charges actuelles de la cellule; représentant des conditions automobiles typiques transitant par une accélération brusque, une décélération, une stagnation du trafic et un fonctionnement sur autoroute. Cette étude vise à comparer la dégradation et la durabilité des FC non hybrides (sans supercondensateur (SC)) avec des configurations hybridées précédemment étudiées, toutes avec les mêmes conditions stoechiométriques et I_{SL} (limite de sécurité actuelle)

Acknowledgments

We would like to thank Professor Stephen Kmiotek for providing us with the opportunity to work with the LRGP team, ENSIC, and the University of Lorraine, and for supporting us throughout the project. We would also like to thank our sponsors at ENSIC, Caroline Bonnet, François Lapicque, and Stéphane Raël, for the project opportunity. We would like to express our deepest gratitude to François Lapicque for his guidance throughout the project, as well as thank Divyesh Arora, Mainak Mukherjee, and Suphaporn Arunthanayothin for their help and support in the lab.

Caroline Bonnet	caroline.bonnet@univ-lorraine.fr
François Lapicque	francois.lapicque@univ-lorraine.fr
Stephane Raël	stephane.rael@univ-lorraine.fr
Divyesh Arora	divyesh.arora@univ-lorraine.fr
Mainak Mukherjee	mainak.mukherjee@univ-lorraine.fr
Suphaporn Arunthanayothin	suphaporn.arunthanayothin8@etu.univ-lorraine.fr

Table of Contents

1.0 Introduction

Fuel cells (FCs) are one of the most promising technologies for diverse transportation applications because of their intrinsic ability to generate electrical power *in situ* while maintaining high operating efficiency [1]. Polymer electrolyte membrane fuel cells (PEMFCs), also known as proton exchange membrane fuel cells, react pure hydrogen and air to produce electricity with emissionless byproducts (water, unreacted gas) and heat [2].

However, there are known issues which arise when trying to utilize a FC in a transportation setting. In general, PEMFCs require a standard 20% excess of hydrogen and 100% excess of oxygen in order to provide a steady power output [18]. This is an economically problematic and wasteful process, but is necessary for a PEMFC to run properly. Another issue becomes apparent when confronting the unsteady nature of the urban car current profile. It is unrealistic to think a vehicle's current profile is constant, and rather has many intense load peaks, generally caused by rapid or inconsistent acceleration/deceleration [3]. Due to physical limitations as well as set safety limitations, the cell is slow to respond to such aggressive load peaks, making a FC alone non-ideal for such a setting. To confront this problem, previous studies have been performed utilizing a FC directly hybridized with a supercapacitor (SC) or batteries, which allows instant current demands to be quickly provided for by the SC instead of the FC [3]. It has been found when confronted with irregular load peaks, a hybridized FC is able to more smoothly transition through the current profile while providing consistent power [3]. Direct hybridization leads to a positive impact on the FC's ability to quickly adapt to high strain loads, however it is unknown how it may affect the membrane electrode assembly (MEA) durability. Additionally, because SC hybridization takes away a lot of strain on the FC, it may be possible to decrease excess hydrogen without experiencing a performance drop [3].

This paper aims to explore the impact of FC hybridization on both the degradation and durability of a PEMFC. In order to understand MEA durability in transportation, the MEA must be aged and degraded in a simulated automotive environment. The European harmonized Fuel Cell Dynamic Load Cycle (FC-DLC) was used, bringing the FC through different current profiles to mimic the energy demand of an urban car. To quantify MEA durability, FC resistances, hydrogen crossover (anode to cathode) and electrochemical active surface area (ECSA) on the cathode were compared after each accelerated degradation. The aforementioned tests can be performed using Electrochemical Impedance Spectroscopy (EIS), cyclic voltammetry (CV), and linear sweep voltammetry (LSV).

2.0 Background

2.1 Basic Fuel Cell Principle

FCs are devices which turn a fuel (e.g. high purity gases) into energy via an electrochemical reaction. Hydrogen oxidation takes place at the anode, and oxygen reduction takes place at the cathode; resulting in water production at the cathode, and a potential difference across the cell that induces the flow of electrons and thus an electric current. Concentration gradients within the cell are the driving force of the reaction. These reactions are often irreversible and the FC will operate continuously as long as the feed gases are supplied and the components within the stack allow for operation.

Overall Reaction: $2H_2 + O_2 \rightarrow 2H_2O$ + Heat

Anode Half (Oxidation) **Reaction**: $2H_2 \rightarrow 4H^+ + 4e^-$

Cathode Half (Reduction) **Reaction**: $O_2 + 4H^+ + 4e^- \rightarrow 2H_2O$

An important comparison to make when investigating the feasibility of FCs in the transportation industry, is the difference between FC and traditional heat engine efficiency. The maximum efficiency, or thermodynamic efficiency, of any FC can be calculated by the ratio of the maximum electrical energy available, which is equal to the change of Gibbs free energy, to the enthalpy of formation, or calorific value, of the overall reaction [6]. For PEMFCs, the thermodynamic efficiency is generally within the range of 62-83%, which is mostly dependent on the phase of water produced (liquid/gas) and the cathode outlet temperature. When compared to the Carnot limit (maximum efficiency for a heat engine) for liquid water and steam below 600ºC, efficiency is on the range of 30-60% [6]. Thus, FCs are more thermodynamically efficient which points to a more sustainable form of energy production.

2.2 Types of Fuel Cells

Sir William Grove assembled the first FC in 1839, then NASA selected PEMFCs for the space program in 1960 because of the safety hazards present with nuclear power systems, and the high cost of solar power systems. FCs powered the Gemini and Apollo missions and were used to supply water and electricity to spacecraft, as well as to lower overall weight by transporting light gases as feed fuels. Despite this early evolution, commercialization of FCs was not explored until the early 1980s, and many factors have limited the marketable development of FCs, including manufacturing cost, fuel generation and distribution and system complexity. A few types of FCs and their respective electrochemical reactions are listed below in **Table 1**. Manufacturing cost is derived from expensive membrane electrode materials and expensive and inefficient fabrication processes (catalyst doping, membrane assembly, etc.). Although the platinum catalyst has a high cost per kilogram, current electrodes for PEMFCs only consist of around 0.2 mg cm^{-2}, which for a 1-kW cell is only about 10 USD [6]. Bipolar plates are also expensive; representing a significant part of the cell cost. FCs also require pure gases as fuel, and especially in mobile contexts there is a lack of availability of refueling infrastructure and impractical storage

techniques. On-board storage of hydrogen is another limitation; however a viable alternative is to reform hydrocarbons such as natural gas, gasoline, or alcohol fuels to produce hydrogen, however, these reformers are large and expensive, and operate at high temperatures. This type of on-board hydrogen production requires a large infrastructure, does not produce totally pure hydrogen, and hydrocarbons still produce carbon dioxide emissions.

Table 1. Summary of the different fuel cell electrochemical reactions [6].

Fuel Cell Type	Anode Reaction	Cathode Reaction
PEM/Acid	$H_2 \rightarrow H^+ + 2e^-$	$\frac{1}{2} O_2 + 2H^+ + 2e^- \rightarrow H_2O$
Alkaline	$H_2 + 2(OH)^- \rightarrow 2H_2O + 2e^-$	$\frac{1}{2} O_2 + H_2O + 2e^- \rightarrow 2(OH)^-$
Oxide	$H_2 + O^{2-} \rightarrow H_2O + 2e^-$ $CO + O^{2-} \rightarrow CO_2 + 2e^-$ $CH_4 + 4O^{2-} \rightarrow 2H_2O + CO_2 + 8e^-$	$\frac{1}{2} O_2 + 2e^- \rightarrow O^{2-}$
Molten Carbonate	$H_2 + CO_3^{2-} \rightarrow H_2O + CO_2 + 2e^-$ $CO + CO_3^{2-} \rightarrow 2CO_2 + 2e^-$	$\frac{1}{2} O_2 + CO_2 + 2e^- \rightarrow CO_3^{2-}$

2.3 Fuel Cell Design

FCs consist of multiple components: two end plates, between which are the two bipolar plates (e.g. anode, cathode), a water channel to maintain constant operating temperatures, then a gas flow plate with a flow pattern (commonly a serpentine regime in parallel to reduce the gas velocity and maximize surface area for mass transfer), and finally a membrane electrode assembly (MEA). A FC stack **(Figure 1)** consists of multiple individual FC units linking each in series to sum the potential across each cell.

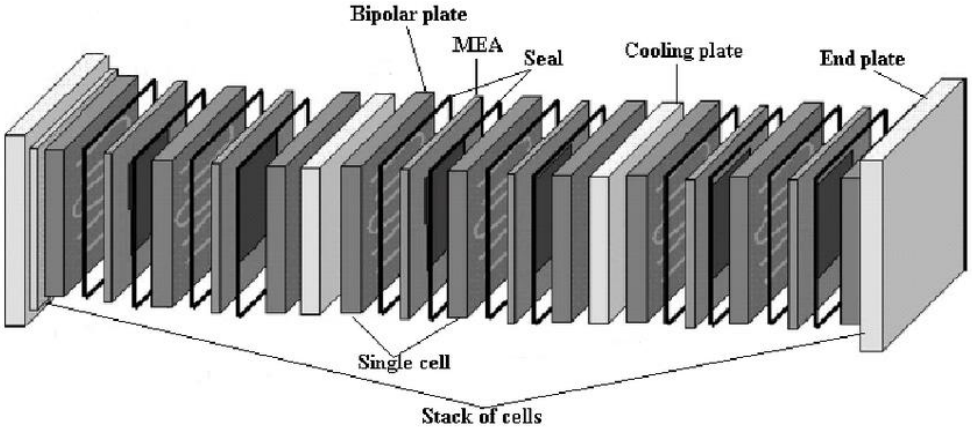

Figure 1. Schematic of Typical Fuel Cell Stack Assembly [12].

2.4 Polymer Electrolyte Membrane Fuel Cells

PEMFCs use a polymer electrolyte membrane (PEM) (typically *Nafion*®), which consists of a sulphonated fluoropolymer sheet around 25-100 μm in thickness. The platinum catalyst roughly has a diameter of 2-5 nm, and is deposited onto (0.4 $mg.cm^{-2}$ and 0.2 $mg.cm^{-2}$ loading at cathode and anode respectively) and supported by a mesoporous carbon-based layer (30 μm thick) [6]. The MEA consists of the PEM layer between a Pt/Carbon sheet on either side. *Nafion*® is chosen due to its comparatively reduce membrane thickness, ultimately improving the FC tightness and thus reducing overall ohmic resistance [2]. The long chain molecules can isolate water with the sulphonated side chains in the polymer to allow for selective and effective hydration [6]. Water management in the FC is critical for PEMFC operation because sufficient water must be absorbed into the membrane to ionize the acid groups as well as to aid in H^+ transport through the membrane via a hydronium (H_3O^+) complex. However excess water can flood the cathode of the FC diminishing performance and limiting power output, and induce washing out of the Pt clusters and carbon particles.

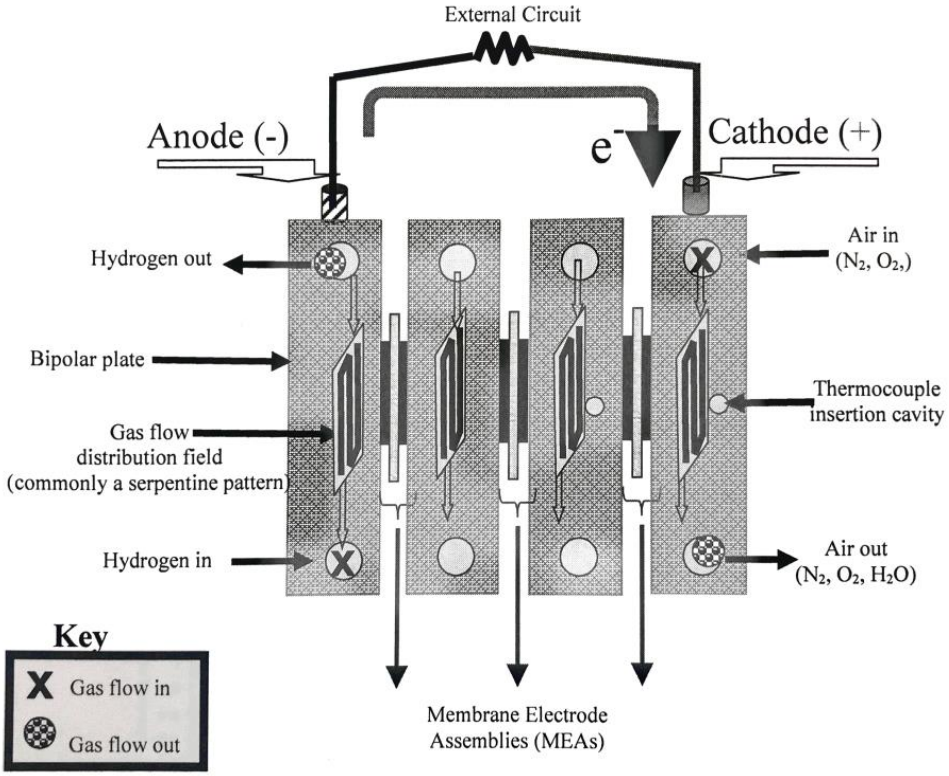

Figure 2. Schematic of Polymer Electrolyte Membrane/Proton Exchange Membrane Fuel Cell.
Hydrogen molecules dissociatively adsorbed at the anode and are oxidized to protons. Electrons travel through an external load resistance. Protons diffuse through the PEM under an electrochemical gradient to the cathode. Oxygen molecules absorb at the cathode, are reduced and react with the protons and electrons to produce water. The product water can either remain within to hydrate the PEM, or travels out of the FC through the cathode and anode exit gas stream [9].

This type of FC utilizes a solid PEM and operates at lower temperatures than other FC types, making it one of the most suitable FC types for diverse applications such as transport (cars,

buses, tramways, trains, aircraft, boats, etc.) [1]. FCs have a relatively high energy density compared to other fuel types, and start-up and shut-down of such systems are controlled with ease by altering feed gas flow [3]. PEMFCs were previously unrealistic for low-infrastructure transportation applications because of the slow response time upstream of the cell (piping, humidifiers), mass flow meters, and sluggish transport phenomena in the cell structure. In other words, rapid acceleration or deceleration of a vehicle causes a large shift in requested power generation and gas flow rates cannot be adjusted instantaneously to suitable levels and attempting to do so can induce losses of energy and efficiency in the transient periods required to balance feed flow rates [3]. Such load peaks induce stress at the cell membrane electrode through a phenomenon known as starvation; a lack of fuel or oxygen within the appropriate locations within the cell [2].

2.5 Faraday's Law

In order to understand how to control and optimize a FC, one must understand how to relate the fuel inlet, consumption and outlet flow rates to the electric potential and current load of the cell. All electrochemical cells operate according to Faraday's law, which states "the amount of a substance consumed or produced at one of the electrodes is directly proportional to the amount of electricity (electrons) that passes through the cell" [6]. Using this relationship, the FC current (I_{FC}) can be directly related to the inlet molar gas flows as seen in **Equation 1**, below.

$$\dot{m}_{gas}\left(\frac{mol}{s}\right) = \frac{I\,(A) * \lambda_{gas}}{mol\,e^{-} * F(\frac{C}{mol\,e^{-}})} \tag{1}$$

Where *I* is the amount of current requested from the cell, *mol* e^- is the amount of electrons given (or used) by the anode/cathode half reactions for 1 mol of gas consumed, λ_{gas} is the stoichiometric factor of the fuel gas and F is Faraday's constant. For PEMFC operation, λ_{gas} is not determined by the balanced chemical equation **(Section 2.0)**, but rather is in excess and thus must be included in the equation [18]. This relationship is essential for understanding FC efficiency and characterization, as well as for precise control of power production in an automotive setting.

2.6 Undesirable Conditions

When starved of fuel, or feed gases (air and hydrogen for PEMFCs), irreversible degradation is caused to the cell, resulting in critical cell voltage drops and hazardous changes to the structural integrity of the FC, as well as the possibility of electrochemical combustion [1]. This generally occurs when hydrogen and air (oxygen) are not given in some form of excess. FC starvation can result in generation of hydrogen in the cathode or oxygen in the anode, or in electrochemical combustion of the carbon catalyst support to form carbon dioxide, which contribute to accelerated decrease in performance and degradation of the MEA, ECSA, and gas diffusion layer (GDL) [1].

As stated before, a lack of hydrogen will cause cell starvation and an inability to provide a steady current. This causes a high anode potential, allowing the water present at the anode to split into hydrogen and oxygen, effectively turning the FC into an electrolyser [6]. The oxygen at the anode can then react with the carbon present in the GDL and backing layers to form carbon dioxide. Similarly, starvation of oxygen causes the reaction at the cathode to produce hydrogen, and the combined presence of oxygen at the anode and hydrogen at the cathode will lead to the reversal of cell potential, inducing electrolysis. Both of these instances result in detrimental corrosion of the catalyst and carbon components in the cell (backing layers), eventually leading to damage or destruction of components [1].

To mitigate such occurrences in dynamic FC applications, an ancillary power source, or energy storage device, such as a battery or SC, can be used to limit or provide current available to the cell. This is especially useful during periods of spontaneous high-power demand (e.g., vehicle acceleration and deceleration) [1]. By coupling, or hybridizing, the FC to an ancillary power source the slow dynamics upstream of the FC and sensitivity of components to sudden power peaks can be mitigated, and allows for smoothed transients in the FC system.

Downstream of standard FC systems and ancillary devices (e.g. battery or SC) are converters necessary to raise the FC voltage to the required level via a DC/DC converter. Additionally, an inverter is then usually integrated into the system for conversion of direct to alternating current. The presence of these ancillary elements results in significant increase in volume, weight, cost and failure risk of the overall system (no risk of failure due to the converter, including control, with reduced energy efficiency) [2]. Since converters are not used in direct hybridization, power losses are reduced. Direct hybridization naturally protects the PEMFC against any fuel starvation phenomena. Additionally, it allows for reduction in hydrogen consumption through the decrease of usual safety levels in the cell e.g. minimum flow rates, excess stoichiometries, and minimum current conditions [3]. During hybridization, cell current can be regulated to a level corresponding to the maximal faradaic current allowed by the flow of fed hydrogen. In other words, in vehicular applications, FCs benefit from being hybridized with an energy storage device that assumes some roles of the FCs. These technologies also significantly optimize the vehicle's fuel economy, emissions, and drivability [1].

2.7 Cycling

In order to simulate an automotive environment, the system was operated under the European harmonized Fuel Cell Dynamic Load Cycle (FC-DLC) [2]. The FC-DLC is an EU standard test protocol developed "for assessing both the performance and durability of Polymer Electrolyte or Proton Exchange Membrane Fuel Cells (PEMFCs) in single cell configuration for automotive applications." [11]. If this protocol is run for roughly 500 hours, it corresponds to an average vehicle utilization of 80 minutes daily over one year or about 16,000 km traveled [11]. The

current density of the cell is varied according to a defined time profile in the range of 0 - 1 A cm^{-2} [2]. To control the FC-DLC load profile, as well as the gas inlets necessary, an in-house software was developed by Stephane Raël using MATLAB-Simulink® **(Appendix 8.3)**.

The same load cycle was used for both FC with and without direct hybridization to one or three SCs. From previous studies [3], it has been found hybridization has led to a smoothening impact on the FC voltage (V_{FC}). Hybridization exponentially smooths the V_{FC} profile by responding to drastic load changes more quickly, giving the FC more time to adapt to the new cycle current **(Figure 3)**. The FC tends to be slow to adapt to new current demands due to the response time of the gas flow meters, as well as time needed to establish steady-state operation.

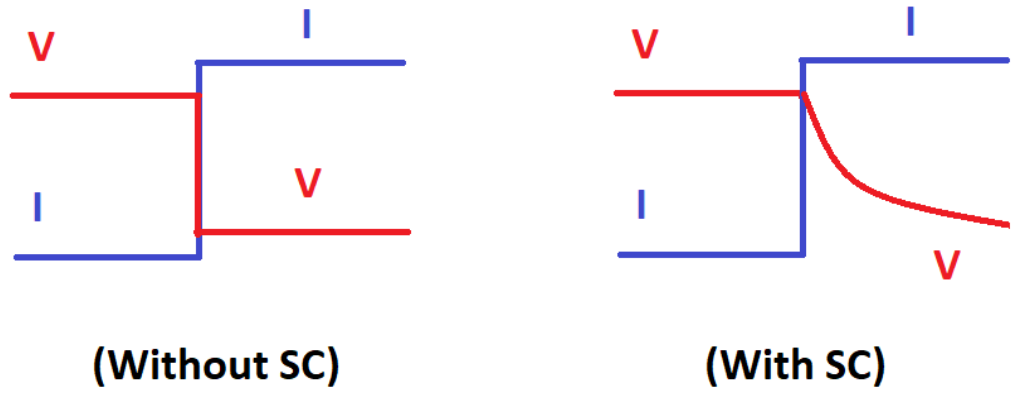

Figure 3. Smoothening of Voltage Transitions.
By directly hybridizing a supercapacitor to the fuel cell, voltage transitions are smoothened during transient current operation. This also helps reduce the total hydrogen supply required by the system, as well as stress on the fuel cell caused by the requested current and sudden changes to the system.

2.8 Electrochemical Characterization of the Fuel Cell

In FCs, performance is fully related to the properties of the interfaces between the different active phases (gases, solids, liquids), and there are many important contributors as it is a multicomponent system (e.g. membrane/anode, membrane/cathode, etc). Each of these factors has an effect on both the resistance and the charge transfer phenomena present within the MEA. It is essential to ensure a homogeneous distribution of pressure at all fastening points on the end plates **(Figure 1)** to ensure a proper connection between layers. In addition, the interface resistivity parameter, which relates the quality of the interface itself, will be influenced by the different layers, the quality and integrity of the layers, as well as the conductive compatibility of the materials in contact. The exchange of charge between the two materials taking place in this zone are limited by a charge transfer resistance. Throughout the lifetime of operation, the system undergoes numerous morphological and chemical changes which can influence MEA integrity. In the course of aging, the MEA materials will experience phase changes as well as dimensions and microstructure that may influence the interface structure [6]. Aged MEAs will tend to have catalytic agglomeration which greatly reduces the active surface area of the membrane [9]. The

manufacturing mode of the electrodes and other components of the MEA can also lead to a fluctuation of the properties of the contact zones between active materials. It is the evolution of these different parameters that we will try to quantify during the phases of characterization. In order to analyze such changes in the MEA, techniques such as EIS, LSV, and CV can be utilized to quantify FC resistance, hydrogen crossover and ECSA respectively.

2.8.1 Polarization Curve

The general performance profile of a FC can be quantified with a polarization curve, which plots the cell voltage as a function of the electrical current density [2]. The polarization curve can also be used to explore the performance of the system based on the current density imposed at a constant stoichiometry. In an aging context, establishing polarization curves before and after the operation of the cell makes it possible to quantify the performance losses. A typical polarization plot is shown in **Figure 4** below.

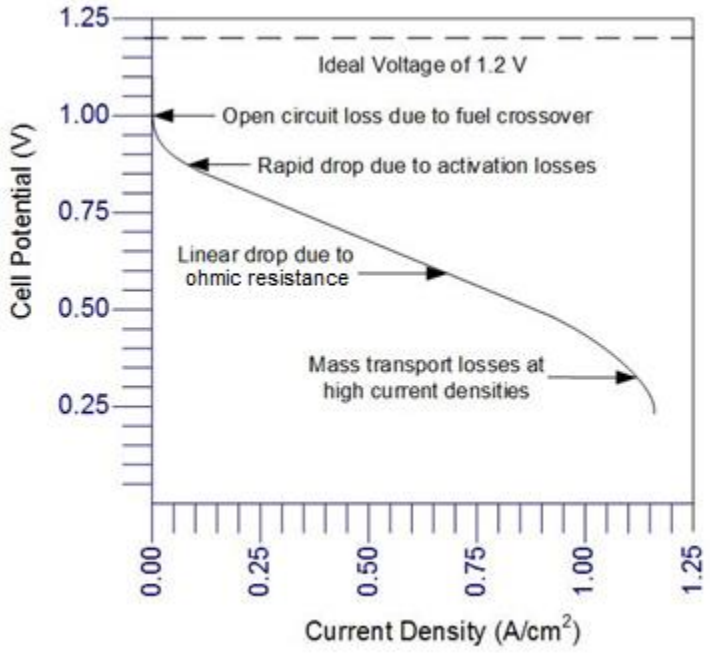

Figure 4. Polarization Plot.

A typical polarization plot is shown, with theoretical cell voltage (ideal voltage) as well as the main sources of losses at various current densities [13].

The polarization curve can be used to elucidate the chemical, physical and electrical phenomena which define the voltage current profile of a FC. The voltage drop, or overvoltage, can be caused by three main physical resistance or limitations [6]. At low currents and thus low current densities, kinetic loss, also known as the charge transfer resistance, is apparent. This is caused by limitations of catalyst activation and by the non-instantaneous reaction kinetics (in particular at the cathode) which result from the rapid voltage decrease from the open cell voltage (OCV) [10]. At intermediate current densities a linear ohmic loss is attributed to Ohm's law (V = IR), which dictates that the ohmic drop within the cell is caused by resistance to electrical flow in the FC

components (may be altered by humidification). The slope of the "linear" portion of the curve may differ from the ohmic resistances because of the other resistances which could be apparent. At high current densities the FC is mainly limited by mass transport losses, which are attributed to the rate at which mass transfer can occur (hydrogen and oxygen flux through the GDL to the catalyst site). As you increase the amount of fuel or oxygen entering the FC mass transfer resistance decreases because you have a larger driving force stemming from the concentration gradients on the two sides of the FC. Mass transfer resistance is more heavily dependent on the oxygen flux because hydrogen, being a smaller gas particle, can more easily diffuse through the GDL and into the MEA. The transport phenomena which limit the reaction within the cell occur in the following steps: transport by diffusion to the catalytic site (concentration gradients, convective flow), mass transfer to the electrode, adsorption, charge transfer and chemical reaction, desorption, and then again transport by diffusion (Fick's law, Navier-Stokes, Ohm's law).

2.8.2 Electrochemical Impedance Spectroscopy

EIS was used to characterize the FC by quantifying both the ohmic, activation and mass transport resistances. Effectively this technique measures the dielectric, or insulative electric, properties of a circuit as a function of frequency [5]. With a set current load, the test will go through a range of alternating frequencies with an amplitude 10% of the set current. Dielectric information is captured in the form of a complex function plotted on a Nyquist plot giving the FC resistive circuit profile. This test is carried out across many different current loads (10-100A) in order to compare how each resistance develops as the FC is required to give more power.

As mentioned previously, the Nyquist plot is the graphical representation of the complex impedance function **(Figure 5)**, consisting of both the imaginary term (Z") vs. the real term (Z') frequencies which are components of the complex function [5]. From the diagram one can discern certain (ohmic, charge transfer and mass transport) resistances by using three characteristic frequencies: high frequency (~1 kHz) governed by ohmic resistance, at intermediate frequency (~22 Hz) governed by the the cathodic capacitive arc, and at low frequency (~100 mHz) governed by mass transport resistances. In order to interpret this graph and produce definitive values in terms of individual resistances, one must use a theoretical mathematical model for the equivalent FC circuit model **(Appendix 8.7)**. The comparison of resistances after periods of accelerated degradation (cycling) can show the trend and rate of FC degradation.

$$Z\ (impedance)\ =\ Z'\ (real\ term)\ +\ jZ"\ (imaginary\ term) \qquad (2)$$

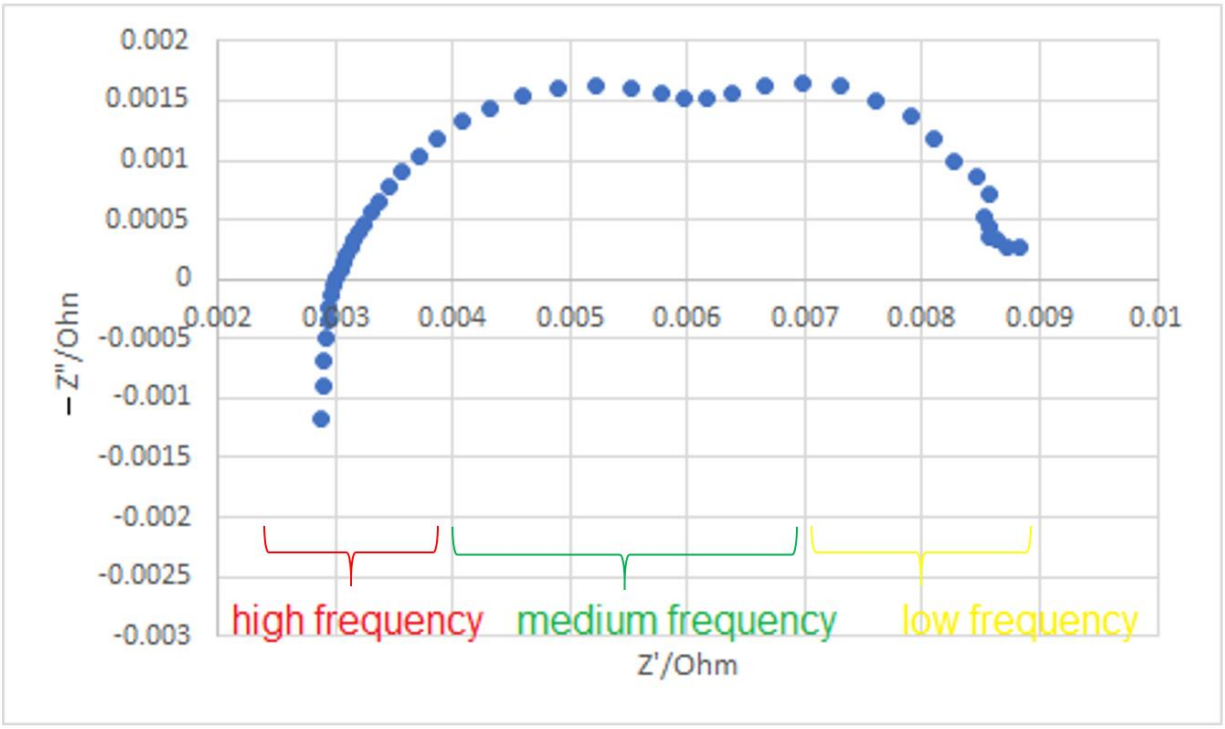

Figure 5. Electrical Impedance Spectrum (Real Part (Z') vs. Imaginary Part (Z'')).

The Nyquist plot expands to the right (low frequency domain) throughout degradation because resistances increase (ohmic, charge transfer, mass transport). EIS is strong technology for providing insight into various charge transfer resistances. Diffusion resistance at the anode is generally not considered because hydrogen is purely at the anode, and transport is so fast the limitation is negligible compared to that of oxygen.

The mathematical basis under which the Nyquist plot functions is:

$$Z = \frac{E_{we}}{I_{we}} = \frac{E + v_a sin(\omega t)}{I + I_a sin(\omega t + \varphi)} = Z_0 * \frac{sin(\omega t)}{sin(\omega t + \varphi)} \quad (3)$$

$$Z(\omega) = \frac{E_{we}}{I_{we}} = Z_0 e^{j\varphi} = Z_0 * (cos\varphi + jsin\varphi) \quad (4)$$

$$Z' = |Z| * cos(\varphi) \quad (5)$$

$$Z'' = |Z| * sin(\varphi) \quad (6)$$

2.8.3 Linear Sweep and Cyclic Voltammetry

Despite the use of resistance, another important part of FC characterization is the analysis of fuel (hydrogen for PEMFC) crossover as well as the ECSA. These two properties are very important to understand when studying FC degradation because they represent both membrane permeability (crossover) and catalyst agglomeration and inactivity (ECSA). LSV is the technique used to measure the quantity of hydrogen which permeates through the membrane. This technique is generally conducted at lower scan rates (~2 mV s^{-1}). A potential is given at the

cathode such that the hydrogen which crosses over through the MEA will deionize (oxidize) and a current will be generated. An inert gas (argon) is used instead of air to purge the FC of any remaining oxygen so the only current generated at the cathode is from hydrogen. An increasing range of potentials are applied at the cathodic site until the current generated plateaus (**Figure 11**).

This linear domain represents a hydrogen permeation limitation, such that the current at this region signifies the max amount of hydrogen crossing over. The hydrogen flux can be found from this max limiting current using Faraday's law. It is expected the maximum current achieved will increase over time as the MEA becomes more porous and more hydrogen can crossover.

ECSA can be measured using another technique called CV. This method allows measurement of the current as the FC is brought through a cyclic upward and downward potential (high to low, low to high) scanning between two potentials levels at a larger scanning rate. The larger scan rate exploits phenomena visible in the transient domain. The acquisition data are plotted on a cyclic voltammogram, in which current is plotted against voltage. From this, a cathodic peak can be discerned at a certain range of potential which represents hydrogen adsorption on to the catalyst. Over time, less hydrogen will be able to absorb onto the platinum catalyst and thus will represent a decrease in catalytic activity.

3.0 Methodology

3.1 Materials

For experimentation a 100 cm^2 PEM single-cell FC was used, with the option of direct hybridization to one, or three, 3000F SCs. This cell's MEA is composed of *Nafion*® 212 50 µm thick membrane, Pt/C electrodes with a 0.4 mg cm^{-2} and 0.2 mg cm^{-2} catalyst loading at the cathode and anode respectively, and 285 µm thick GDLs including a macroporous and a microporous layer on carbon fiber paper [2]. Two water tanks were used to humidify the inlet gases (hydrogen and air) depending on the experimental configuration. Two voltage probes have been installed in the circuit for monitoring of both fuel cell and, when hybridized, the SC potential. Additionally, one Tektronix® current probe was also installed for monitoring the FC load (I_{FC}). SC current was simply calculated from the measured load and cell currents [2]. A complete list of equipment is listed in **Appendix 8.1**.

3.2 Experimental Setup

There were multiple experimental configurations on the test bench **(Figure 6)** depending on which test was being carried out. For this study there were three individual setups which covered, cycling, EIS characterization, and LSV/CV characterization. Each of these configurations have either different physical connections on the bench, different equipment attached or different inlet gas conditions.

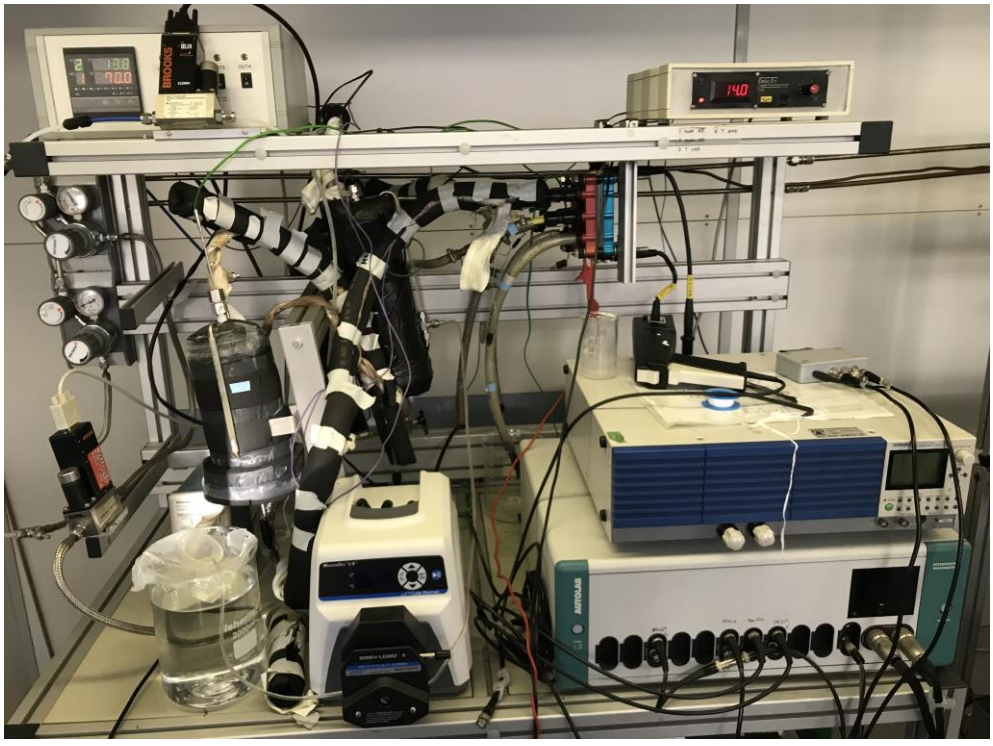

Figure 6. Test Bench Setup in the SysPol LRPG Lab at ENSIC, Universite de Lorraine.

3.2.1 Cycling Configuration

While undergoing the FC-DLC **(Section 2.7)** , the FC load (Kikusui) and inlet gas flow rates are controlled by the Controldesk® MATLAB interface with a dSPACE® card **(Appendix 8.4)**. Controldesk® uses the set reference load (I_{Ref}) to determine the inlet gas flow rates. In the event the measured FC load (I_{FC}) drops below I_{Ref} Controldesk® will reference the safety limit current (I_{SL}) to determine the inlet gas flows. When the FC is hybridized to a SC, Controldesk® will reference I_{FC} for the inlet gas flow rates as I_{Ref} is the summation of I_{SC} and I_{FC}. The gaseous streams were set to supply the FC at stoichiometric coefficients of $\lambda_{H2} = 1.2$ and $\lambda_{Air} = 2.5$. The air humidifier (V-102) was maintained at 44 ºC while the FC (R-101) was maintained at 55 ºC. From the outlet of V-102, air is 100% humidified and thus partial pressure is equal to the saturation pressure. A heating element and insulative jacket was installed on the connecting tube between V-102 and R-101 (Stream 9) which was set and controlled to 70 ºC. From this the air is assumed to reach the inlet of R-101 at roughly the same temperature (~55 ºC) making the relative humidity of the inlet air roughly 55%. The fuel line (Stream 1) remained dry, by-passing the hydrogen humidifier (V-101) and entering R-101 (Stream 7). All equipment and streams are portrayed in the process flow diagram (PFD) **(Figure 7)** and the process and instrumentation diagram (P&ID) **(Figure 8)** below.

3.2.2 EIS Configuration

When setting up the test bench for EIS characterization, alternative equipment (computer, potentiostat) must be attached for proper control and data acquisition. The fuel flow rates and FC load are still controlled by the Controldesk® interface. The gaseous streams were continued to be supplied at $\lambda_{H2} = 1.2$ and $\lambda_{Air} = 2.5$. EIS requires an alternating current (AC) in addition to the DC provided by the Kikusui load. For this the Autolab **(Figure 6)** potentiostat is connected to the test bench. The operating conditions for the inlet gases remain the same with dry hydrogen and air at 55% relative humidity.

3.2.3 LSV/CV Configuration

LSV/CV characterization tests are run after completing the EIS characterization, so both operating conditions and the test bench configuration must be changed. During this characterization, no load is requested but rather a potential is placed on the FC. Specifically, during CV, a load has to be requested and accepted due to the nature of the test. To do this a booster is used over the load, because it is able to both request and accept current generated by the FC. The hydrogen line (Stream 7) is disconnected to be replaced by the humidified hydrogen line (Stream 6). The Stream 5 three-way valve is switched so the fuel gas is no longer by-passing V-101. The air and hydrogen thermostated water baths (E-101/E-102 respectively) are both set to 60 ºC to increase the temperature of V-101 and V-102 to roughly 55 ºC. This is done to ensure both gas streams are entering R-101 at 100% relative humidity. Additionally, the Stream 8 three-way valve is switched allowing for argon (Stream 3) to pass through the FC instead of air. As a result of no load being requested from the FC, Controldesk has no current to reference for the

inlet flow rates for argon and hydrogen. Thus, manual flow rates are set at 300 STP mL min^{-1} for both gases. Once setup is complete, the bench must be left for about 45 minutes to ensure all operating conditions are at steady-state as well as to allow enough time for the argon to purge the FC off all remaining oxygen.

3.3 Process Diagrams

Process flow and process and instrumentation diagrams for the PEMFC system (**Figure 6)** are shown below (**Figures 7 and 8)**. The shown diagrams are in the cycling configuration **(3.2.1)**, however the modifications for alternative configurations are described above **(3.2.2 - 3.2.4)**

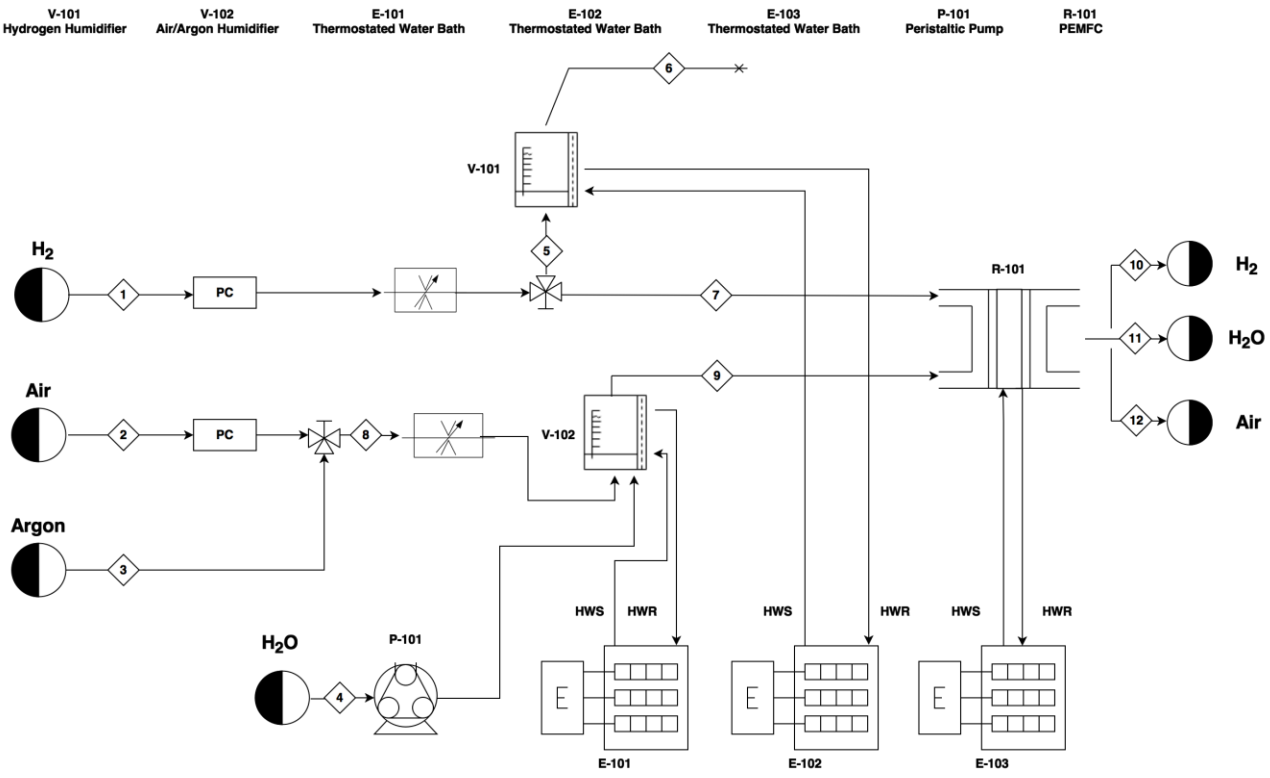

Figure 7. Process Flow Diagram for Cyclic Operation.

In this process configuration, hydrogen bypasses the humidifier and air passes through the humidifier, both subsequently supplied to the fuel cell.

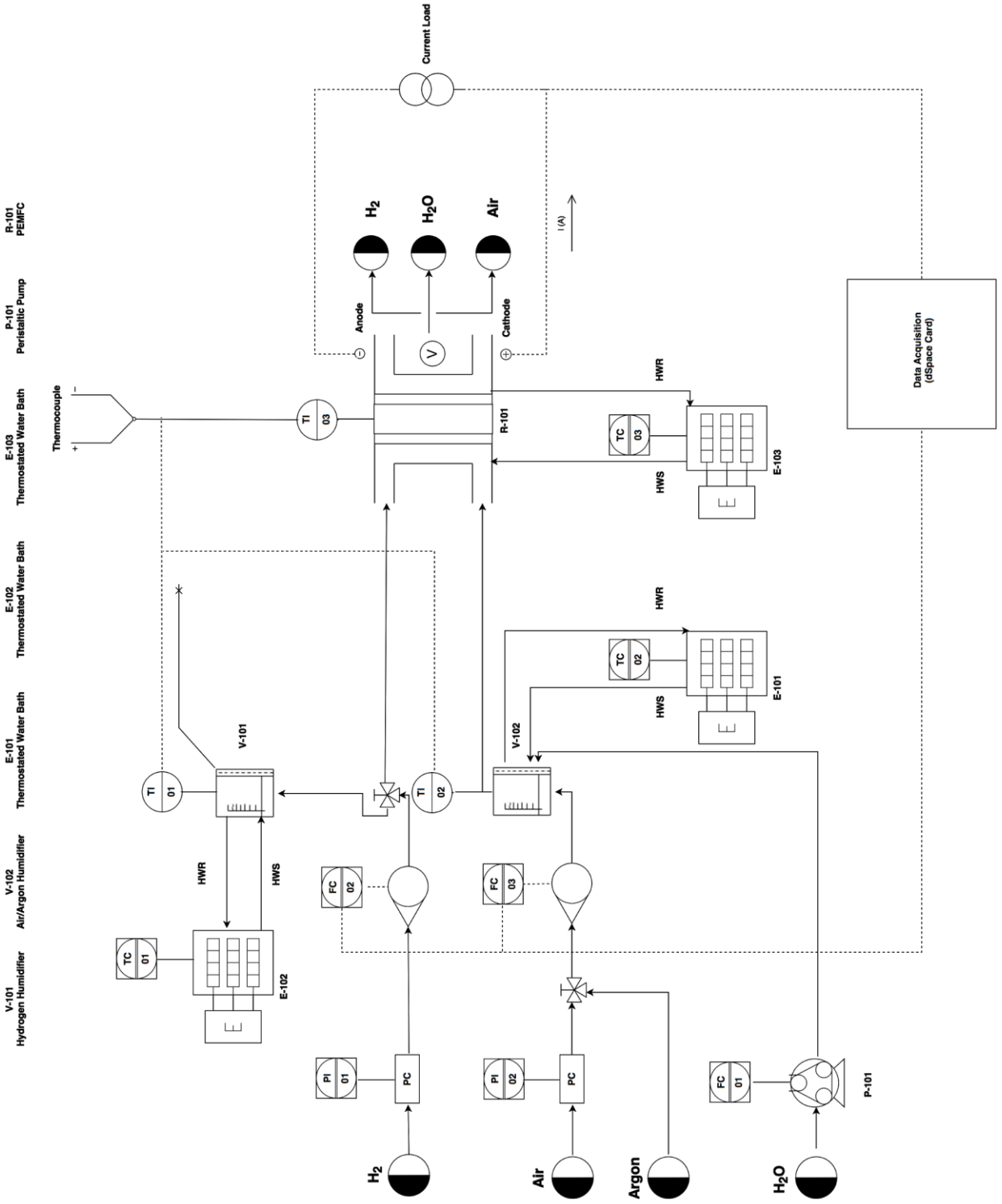

Figure 8. Process and Instrumentation Diagram for Cyclic Operation.

In this configuration it is visible that the flow meters and thus reference current are directly controlled via computer. All temperatures are monitored via thermocouples and temperature display can be cycled through via a dial. Water bath temperatures and flows are also regulated.

3.4 Experimental Trials

Outlined below are is an overview of the test and protocols performed, as well as the experimental design and methods to illustrate how all data was captured and processed throughout the two month period.

3.4.1 Cycling Testing Conditions

As mentioned before, the FC-DLC **(Section 2.7)** cycling protocol was used to simulate an automotive environment which brings the FC through two different domains **(Figure 9)** of urban driving. The UDC, or urban driving cycle is meant to simulate everyday city driving whereas the EUDC, or extra urban driving cycle simulates highway power demands.

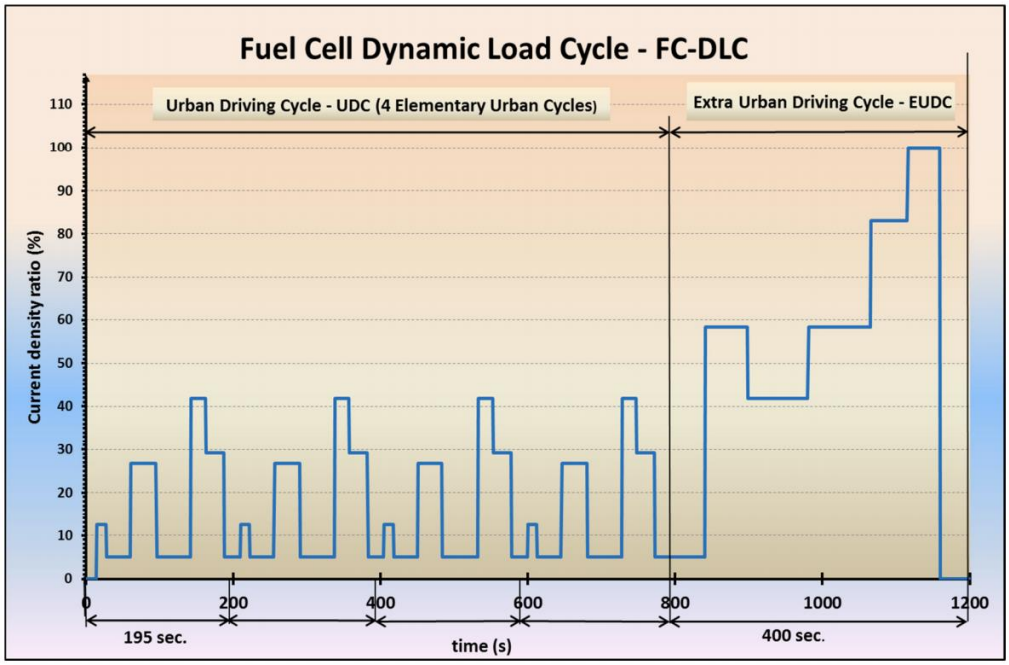

Figure 9. Fuel Cell Dynamic Load Cycle.

This portrays the the two automotive domains of the European harmonized dynamic load cycle which the FC is brought through when cycling [11].

Throughout the FD-DLC, the FC (or FC+SC if hybridized) is brought through a cycle current (I_{cycle}) range of 0.1 A cm^{-2} to 1 A cm^{-2}. It is important to note, the FC had to be be first matured after installing a fresh MEA before starting cycling. Maturation involves requesting a load of 1 A cm^{-2} for at least 24 hours. A characterization is then performed before commencing cycling (0 h). For FC hybridized with a SC, an initial 100 h of cycling is done and then the FC is hybridized. Cyclic operation is employed as an accelerated aging method, and after approximately every 100 hours characterization (EIS, LSV, and CV) is repeated to evaluate the durability and performance of the FC. When considering durability, it is the amount of time, or life span in which the FC can continue to perform within a determined range. For the SysPol LRGP lab at

ENSIC, the FC is not considered degraded until the power performance at maximum power (80A) falls below 20% of its initial performance.

Although cycling is mostly used as a protocol to degrade the FC rather than an experimental test, durability information can be discerned from the acquisition data. Controldesk® records all pertinent cycling parameters, such as the reference and measured FC voltage and current **(Figure 10)**, as well as the measure voltage and current of SC when hybridized. Each of these data points are registered every 100 ms for a total single cycle time of 20 minutes. Due to the vast amount of cycling data collected (roughly 2000 cycles performed for FC lifetime), MATLAB was used to automatically parse through all data points. From this, quantitative durability trends such as FC voltage decay and hydrogen consumption over the FC duration can be found. In the present investigation, these trends were found for a single cell FC without SC hybridization at an I_{SL} of 0.05 A cm^{-2}. These results were then compared to previous studies [3], which used single cell FC configurations hybridized to one or three SCs, each with a 3000 F capacitance, at an I_{SL} also set to 0.05 A cm^{-2}.

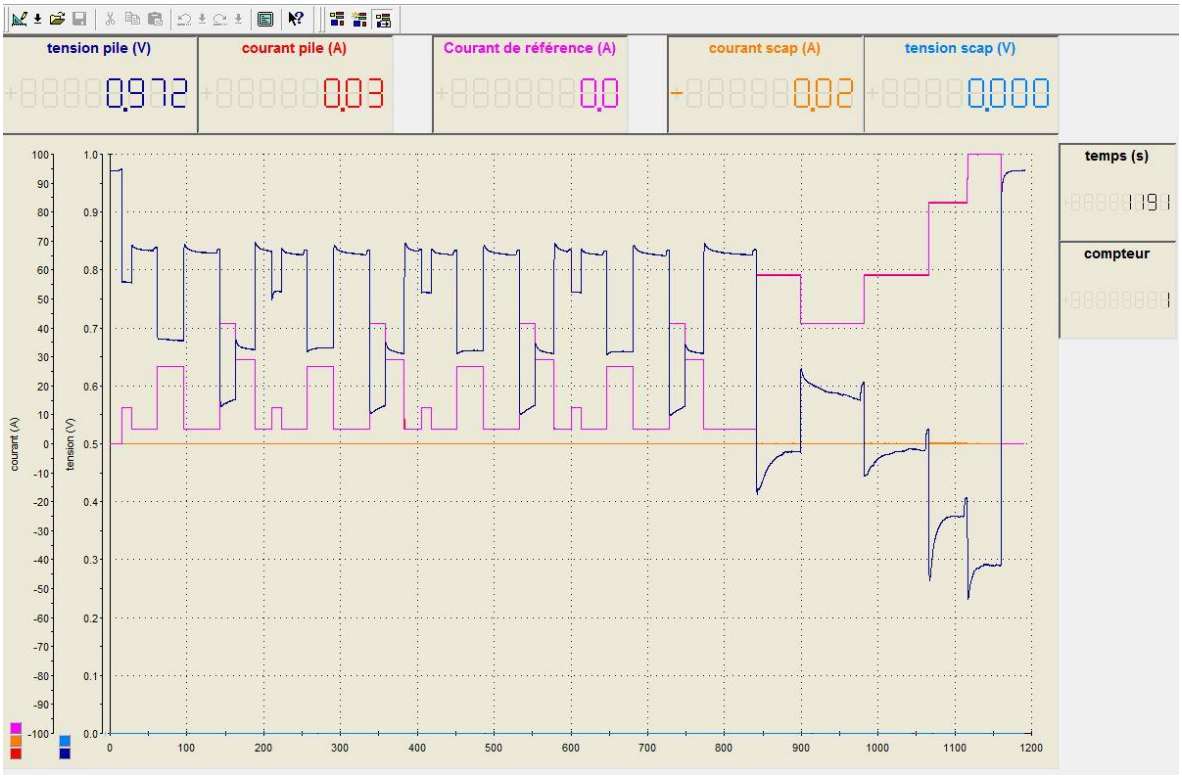

Figure 10. Cycling operational measurement using the Controldesk interface.
Developed in-house by Stephane Raël using Matlab-Simulink®. The fuel cell voltage (navy), fuel cell current (red), and reference current (pink) are displayed with respect to time. This cycle is without a directly hybridized SC. One cycle requires approximately 20 min for completion.

3.4.2 EIS Testing Conditions

For EIS, all data was measured and collected using the Autolab Electrochemical potentiostat and NOVA software respectively. The operating conditions for the experiment were set to the EIS configuration outlined in **Section 3.2.2**. Experimental spectra were established for 50 points (5 decades, thus 5 orders of magnitude) logarithmically distributed between 100 mHz and 10 kHz. The potentiostat is combined with a module for polarization curve and impedance spectroscopy measurements, and the maximum current range is extended with the Kikuisu charge. For EIS, each test was carried out on a range of current densities between 0.1 - 1 A cm^{-2}. The first test performed was a chronopotentiometry, in which the voltage is monitored with a fixed current for 10 minutes. Following this, the impedance measurements are carried out with both the DC and AC, at an amplitude 10% of the DC, for frequency range of 10 kHz - 0.1 Hz. Show below **(Table 2)** is the experimental design for EIS.

Table 2. EIS Experimental Design.

DC (A)	AC Amplitude	Duration of Chronopotentiometry (s)	Trials Run
10	1	300	1
20	2	300	2
40	4	300	2
60	6	600	2
80	8	600	2
100	10	600	2
110	*NA*	300	1
120	*NA*	300	1

From the chronopotentiometry, FC potential data collected for each current density was processed in order to get the polarization curve (**Figure 16**) and power performance. Data collected from the impedance cannot initially be used because it is in a complex form. Using the mathematical resistance equation for a Warburg equivalence circuit **(Appendix 8.7)**, the obtained data can be fit to the model using Excel to produce quantitative FC resistance values. Both the power performance and impedance of the FC are measures of the durability of the FC.

3.4.3 LSV/CV Testing Conditions

The LSV/CV experiments were run in accordance to the LSV/CV configuration outlined in **Section 3.2.3**. Once the test bench has reached the specific operating conditions, the first test

performed is LSV. As mentioned previously, this technique is used to measure the quantity of hydrogen permeation through the membrane by monitoring electrochemical activity, in the form of a current, by controlling the potential of the cathodic side in the FC [19]. The potential placed on the cathode is scanned from 50 mV to 600 mV at a rate of 2 mV s^{-1} [8]. The test is then terminated, since for voltages above 500 mV oxidation of the carbon catalyst support occurs, and the current value at the plateau region is recorded. From this current, the flux of hydrogen can be calculated using Faraday's law **(Section 2.5)**. The fuel crossover can be compared between a FC with and without direct SC hybridization to observe if SCs aid in the increase of FC lifespan. More specifically, if the addition of SCs help decrease the rate of membrane thinning. An example of a LSV plot is shown below in **Figure 11**.

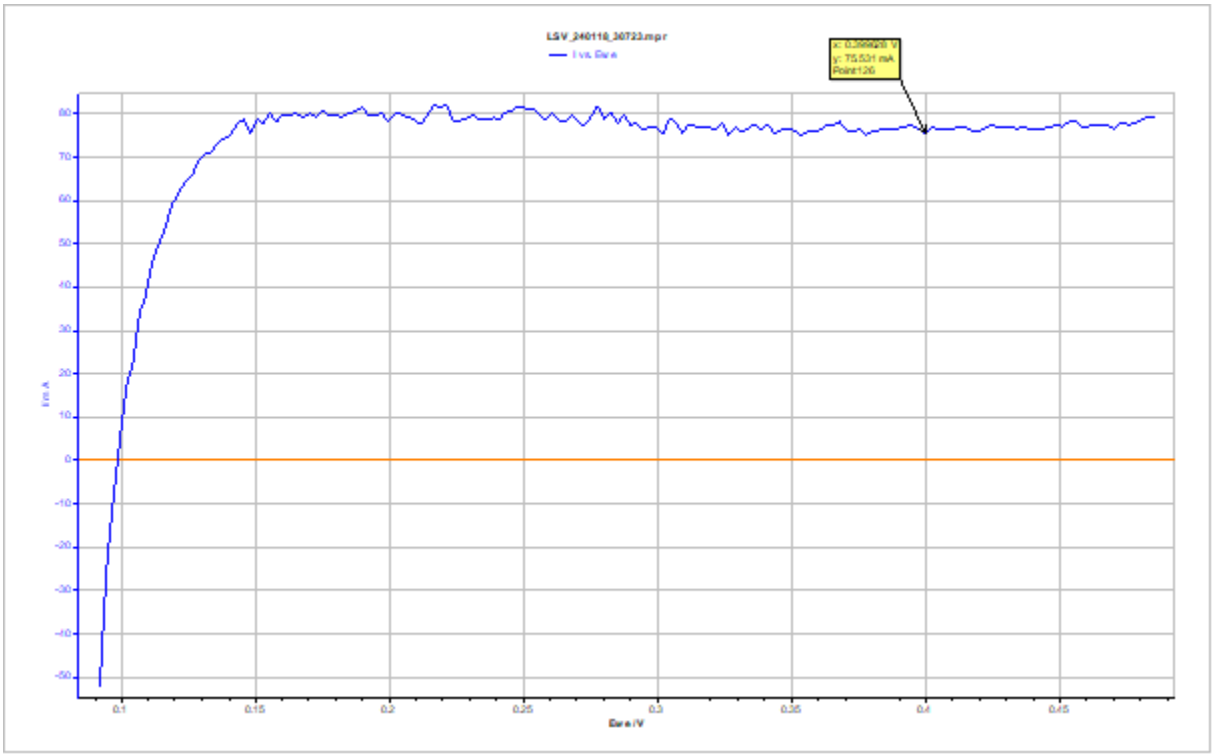

Figure 11. Linear sweep voltammetry (LSV) Plot.
This is a plot of current (mA) versus potential placed on the cathode (V). The region in which the trend does not change (plateau) is the maximum current (limited by hydrogen flux) produced by hydrogen oxidation (deionization) at the cathode.

The next test run in the LSV/CV bench configuration was CV, which is used to calculate the ECSA. Experiments were run between 50 mV to 600 mV at a scan rate of 30 mV s^{-1} [2]. In this technique, the current of the system is recorded while the potential scans between the lower and the upper limit of the potential range considered. From the data acquisition, a cyclic voltammogram (current (mA) vs. potential (V)) graph is generated. During the positive current scan, there are two anodic peaks (shaded in blue **Figure 12**), which corresponds to the adsorption of protons onto the catalyst ($Pt + H^+ + e^-$ -> Pt-H) [19]. Inversely during the negative current

scan, the observed cathodic peak represents the oxidation of adsorbed hydrogen (Pt-H -> Pt + H^+ + e^-) [19]. From the anodic peak, the charge can be calculated using **Equation 7**, and the ECSA can be calculated using **Equation 8**. An example CV plot is shown below in **Figure 12**.

$$Charge\ (C) = \frac{anodic\ peak\ (mAV)}{scan\ rate\ (\frac{mV}{s^{-1}})} \tag{7}$$

$$ECSA\left(\frac{cm^2\ Pt}{cm^2\ S_{tot}}\right) = \frac{charge\ (C)}{210\ (C.cm^{-2}Pt) \cdot S_{tot}\ (cm^2)} \tag{8}$$

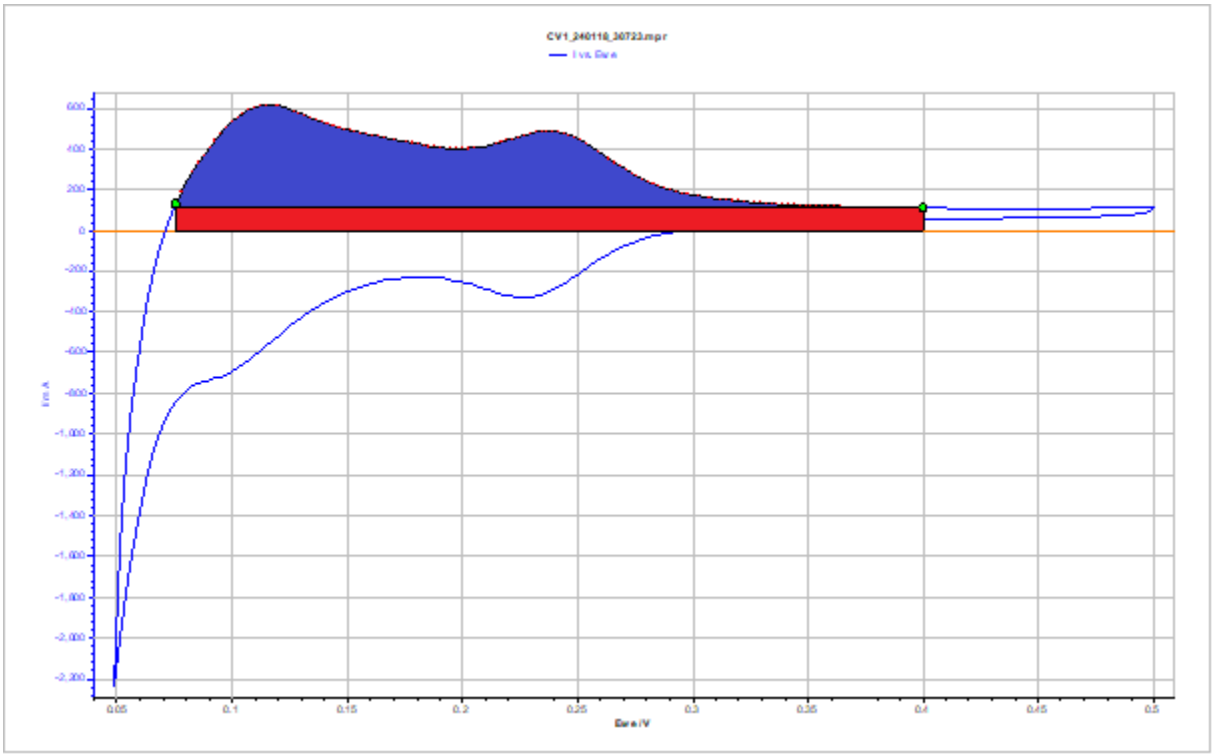

Figure 12. Cyclic Voltammogram.

This graph represents a forward and backward potential scan between the upper and lower limits of the potential range. The positive (anodic) and negative (cathodic) peak represent the adsorption and desorption of hydrogen on to the catalyst. The blue shaded area gives us the charge of the anodic peak when integrated.

4.0 Experimental Results and Discussion

From the experimental trials run **(Section 3.4)**, a large amount of raw data was collected which required processing using softwares such as Excel for curve fitting and MATLAB for parsing through cycling data. All results discussed will be comparing a single cell FC with zero SC at an I_{SL} at 5A to a single cell FC directly hybridized with one and three SCs at the same I_{SL}. All durability comparisons were done in such a way that no result differences could be attributed to the any discrepancies between the initial membranes of each FC. In fact, based on the experimental design, all durability differences are assumed to be due to the addition of a SC. The ultimate goal of this discussion is to comment on the impact of directly hybridized supercapacitance on the degradation and overall durability of the FC using different methods such as V_{FC} decay, power performance, and the rate of change for resistances.

4.1 Cycling Results

As mentioned in **Section 3.4.1**, cycling data was collected over the course of the two month experiment, and three MATLAB scripts (developed in-house) were used to parse through the data set and analyze the evolution of the FC current (mean, minimum, maximum), voltage (mean, minimum, maximum), yield (Wh/L), power yield (W), and hydrogen consumption with respect to cell lifetime. For this analysis we focused on two current densities, 0.2 A cm^{-2} and 0.8 A cm^{-2}, because they best represent the charge transfer and mass transport limitation domains, respectively. Purley based on the number of cycles the FC was able to operate, the FC with 3SC survived the longest at about roughly 4000 cycles, 1SC at about 3700 cycles and lastly 0SC at about 2100 cycles. Although this initially shows a longer lifespan for FCs which are hybridized, the comparison is further investigated using other analytical methods.

4.1.1 Voltage Decay

For analysis, the voltage decay of the FC as a function of time over the total period of cycling can be used to estimate the mechanism of degradation. The mean (V_{FCmean}), minimum (V_{FCmin}), and maximum (V_{FCmax}) FC voltages were recorded (**Appendix 8.6**) and were used to estimate and compare the rate of decay under the various operating conditions. For a FC without hybridization, the rate of decay for V_{FCmax}, V_{FCmin}, and V_{FCmean} was 15 μV h^{-1}, 300 μV h^{-1}, and 98 μV h^{-1} respectively during 100 h to 680 h of operation. During the last hours of operation, the decay was much more pronounced, the value of V_{FCmax} increased 12 times for and V_{FCmin} increased 5 times. The reason for such a variation during the last hours of operation of the cell can be attributed to the mechanical fatigue of the MEA.

These values are compared to a FC with direct hybridization to 3 SCs, resulting in 25-30 μV h^{-1}, 100 μV h^{-1}, and 60 μV h^{-1} for V_{FCmax}, V_{FCmin}, and V_{FCmean} respectively, during 100 h to 1200 h of operation. For the last 150 h of operation, from 1200 h to 1350 h, the rate of decay intensified. During this time frame the V_{FCmax} increased 3 times and V_{FCmin} increased 4.5 times compared to

the initial decay. The values for voltage decay throughout the majority of the cell life for the FC directly hybridized to 3 SC, and for the non-hybridized FC are summarized in the table below.

Table 3. Overall Voltage Decay.

Rate of Decay for:	FC+0SC (t = 100 h to 680 h)	FC+3SC (t = 100 h to 1200 h)
V_{max}	15 μV h^{-1}	25-30 μV h^{-1}
V_{mean}	300 μV h^{-1}	100 μV h^{-1}
V_{min}	98 μV h^{-1}	60 μV h^{-1}

For the directly hybridized cell, the overall V_{FCmean} rate of decay was lower than for that of the non-hybridized mode, because, in the hybridized mode the reference current for any instantaneous moment in the cycle is equal to the FC current plus the SC current, rather than directly equal to the FC current. This means that during regions of cycling that request lower currents, and thus higher voltage, the cell spends more time in potential ranges (0.7-1 V) in which the MEA is prone to accelerated corrosion of the carbon catalyst-support [15] (**Figure 13)**. In the hybridized mode, the SC is able to provide voltage to offset these peaks while the FC adjusts its flow parameters, so the catalyst spends less time in a degradative domain. This is a potential explanation for the increased durability of the cell with hybridization.

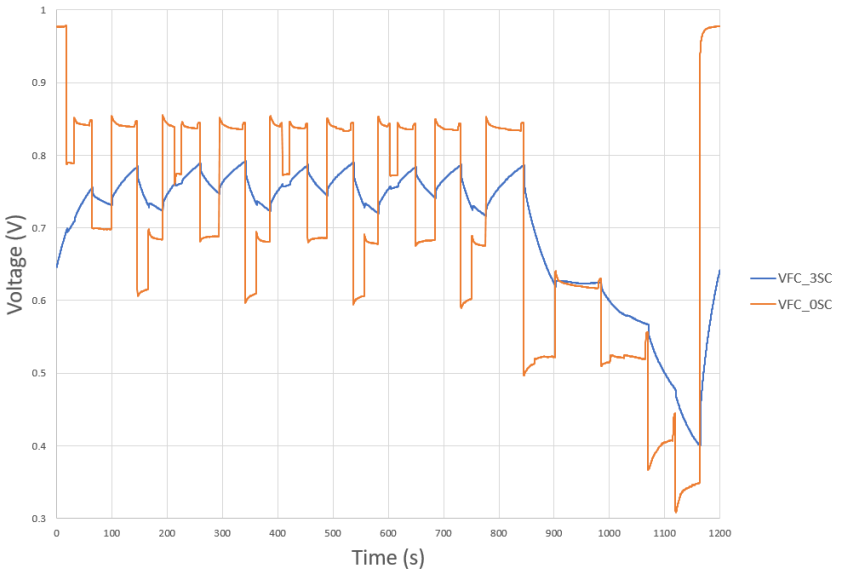

Figure 13. Voltage vs. Time for One Cycle.
A comparison of fuel cell cycling operation with direct hybridization to three supercapacitors, and without hybridization. The supercapacitors cause a smoothening effect, lowering maximum voltage peaks, thus increasing the durability of the cell.

The voltage decay throughout the lifetime of the non-hybridized fuel cell can also be seen below (**Figure 14)**, at three different cycling currents (26.7A, 83.3A, and 100A). Cycling currents roughly below 30A correspond to a high (> 0.7V) FC potential, which could lead to accelerated carbon support degradation. The rate of voltage decays for each of the three different cycling currents for the non-hybridized mode were then compared to the fuel cell hybridized with 3SC. Significant decrease in the voltage decay rate was found for the hybridized FC; for 26.7A, 83.3A and 100A, the rate of decay decreased ~48%, ~35%, and ~57% respectively.

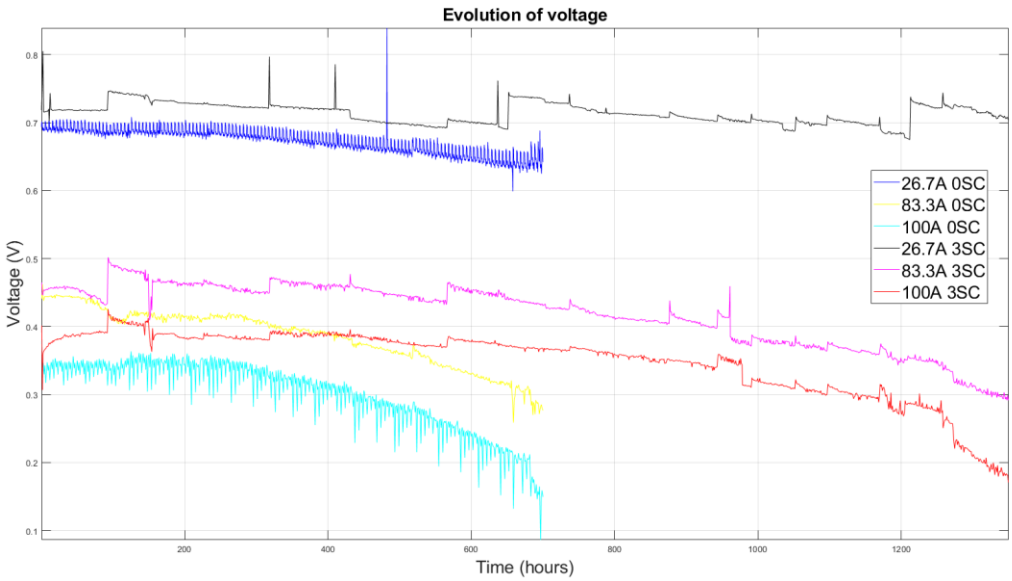

Figure 14. Evolution of Voltage for lifetime of cell.
Voltages for three different cycling currents (26.7A, 83.3A, and 100A) are shown as a function of time.

4.2 Polarization Curve and Power Performance

From data acquired using EIS **(Section 3.4.2)**, the FC potential could be plotted against the current density for each ~100h characterization over the two month study. This plot gives the polarization curve **(Figure 15)** of the FC which is useful to visualize the basic voltage decay trend per current density. It was noticed for the FC without hybridizaiton, there was a steady decrease in FC potential per current density over the last 350 hours.

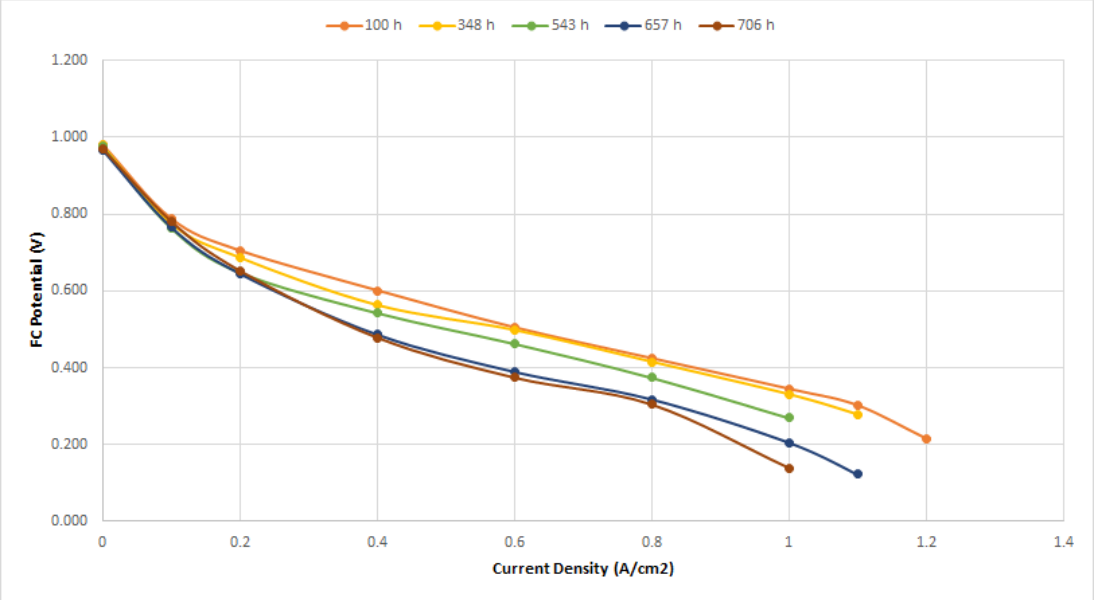

Figure 15. Polarization curves over 0SC FC lifespan.

Although polarization curves are a known feature to observe degradation trends of a FC, difficulties arise when trying to compare such trends to other experiments (i.e. FC hybridized to SCs). It is difficult to compare visually due to the clutter amounted from the series, as well as it is difficult to quantify differences between the curves. As a result, power (W) **(Figure 16)** and power performance (% change from initial over lifetime) **(Figure 16)** were compared, which gave a much better idea of how SCs impacted the durability of the FC. In order to calculate power, the FC potential data was multiplied by the respective currents for each ~100h characterization. It is important to note, the first 100h of cycling for all FCs (0SC, 1SC, 3SC) are done without hybridization. Thus, in order to compare the impact of SC hybridization, all comparisons made over the lifetime of the FC start at 100h instead of 0h.

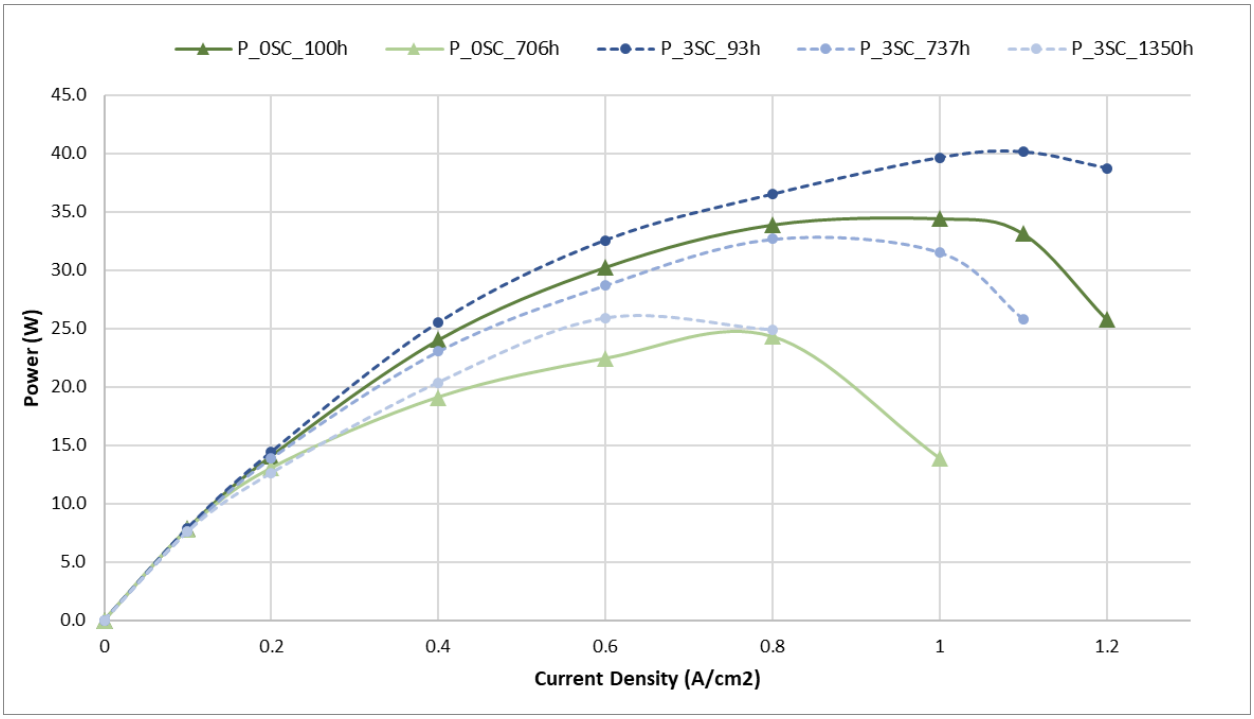

Figure 16. Power (W) vs. Current Density (A cm^{-2}).
This graph compares the power profile between a FC with and without hybridization to three SCs. The series plotted are beginning and end time intervals for the non-hybridized FC, and beginning, middle and end time intervals for the hybridized FC.

When graphing the power against current density for beginning, middle and end intervals, a clear degradation can be visualized. As shown in **Figure 17**, the difference in the power profile and overall power production from 100 h to 700 h for the FC without SC is substantial. However, it is noticeable the 100 h characterization for the 0SC FC configuration has an overall lower power performance than that of the 3SC FC. This means the membranes are not completely comparable because up to 100 h of cycling both FC were cycled without SCs, and thus should show a similar power profile.

When comparing the same profile for a FC hybridized to three SCs, there is a much smaller power decay between 100 h and 700 h. For the 0SC FC, the last (end of life) characterization was at 706h, however the 3SC FC was not only able to last nearly 2x longer, its power profile at 1350h was still slightly higher than that of the 0SC FC at 706h. The decay difference between 0SC and 3SC is best shown when comparing the percent power degradation from the initial (100h) characterization, which is an arguably better way to compare the configurations as it eliminates bias from any membrane differences **(Figure 17)**.

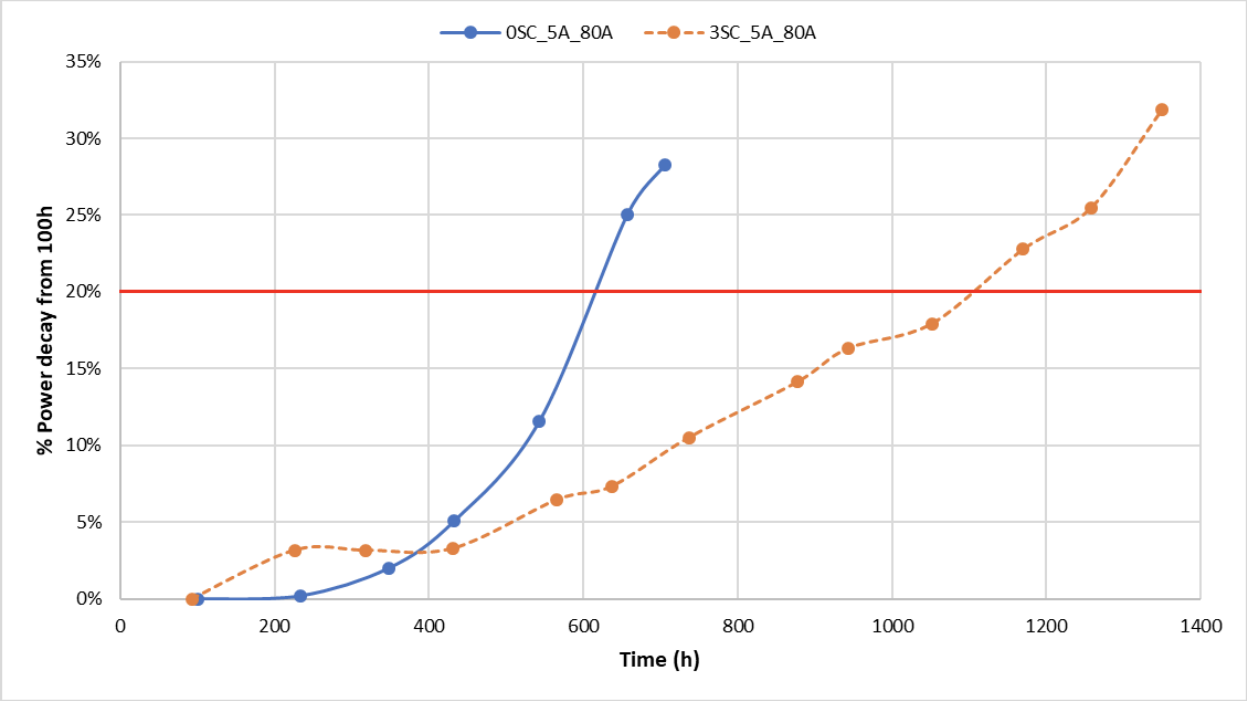

Figure 17. Percent Power Degradation vs. Time (h).
This graph portrays the percent maximum power decay from the initial 100h characterization for both non-hybridized and hybridized FCs. The horizontal red line represents this studies set degradation limit for a FC, where it is producing 20% less maximum power then its initial maximum power.

As mentioned previously **(Section 4.4.1)**, the FC is considered degraded (end of life) when its maximum power output has decreased by 20% from its initial (100h) output. For both 0SC and 3SC FCs, the maximum power was achieved at a current density of 0.8 A cm^{-2}, which made it easier to compare power degradation profiles. From **Figure 17**, it is clear the non-hybridized FC surpassed the 20% power decay limit in roughly 50% of the time it took the 3SC FC. It is also observed when the 0SC FC hit 20% power degradation, the 3SC FC was only at 7%. It is thus evident the addition of SCs through direct hybridization improved the FC's power durability significantly, extending its usable lifetime. However, because there are many factors involved in FC operation, the precise reason to why power durability was improved cannot determined from this test alone. One possibility to why durability has been improved could be due to the decrease in catalytic corrosion (when hybridized), which is caused by high V_{FC} domains and rapid power demands. This idea will be further discussed in comparison with other test results to justify its hypothetical integrity.

4.3 Electrochemically Active Surface Area

Using the data acquires from CV **(Section 3.4.3)** the ECSA of the catalyst in the FC MEA could be calculated. When correlated with each characterization, a plot could be made over time to observe the decay of ECSA for a FC with and without (1,3) SC hybridization **(Figure 18)**. Using an Excel linear regression technique **(Table 3)**, one could roughly determine the rate of decay

[cm^2 Pt / (cm^2 electrode)*(h)] for each FC configuration. For ECSA, you are only able to compare trends versus values because each membrane was unique in the amount of initial cm^2 of Pt per cm^2 of electrode.

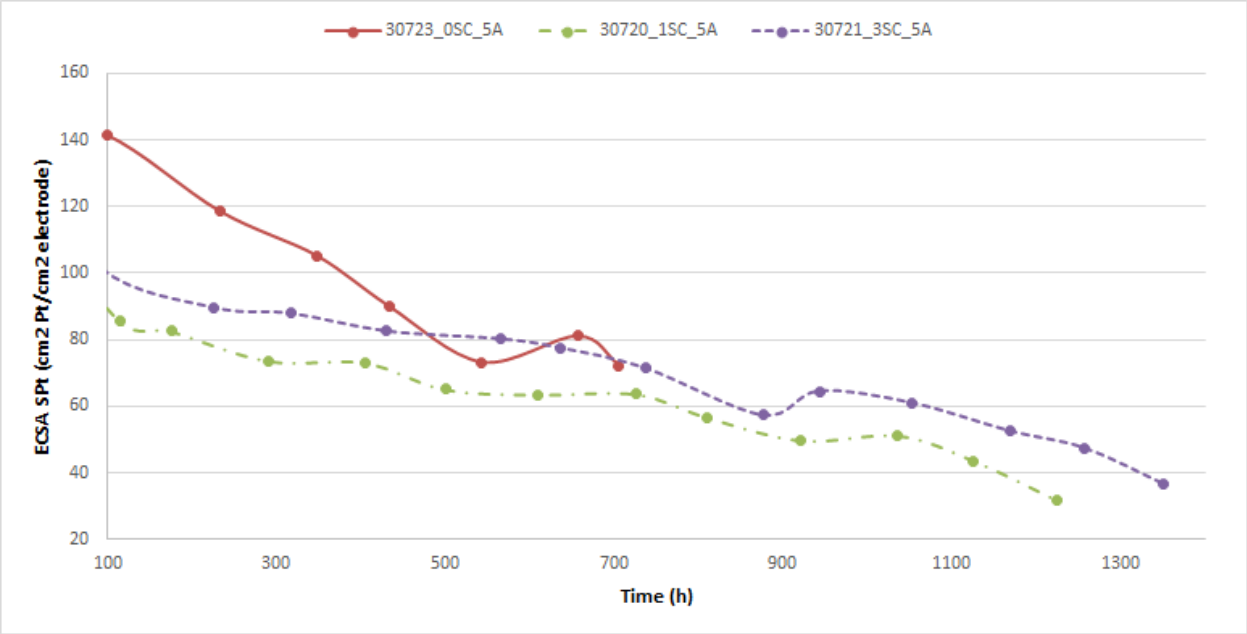

Figure 18. Electrochemical active surface area (ECSA) vs. Hours of Cycling (h).
This graph compares the overall ECSA trend over the lifetime of the FC. A linear regression was used in order to quantify the change of ECSA, but is realistically not the precise rate of decay.

Using the slope of the trend from the linear regression, the ECSA rate of decay for a FC with 0SC was found to be ~160% higher than that of a FC with 1SC and ~140% higher than that of a FC with 3SCs. The decay value and respective standard deviations in those values can be found in **Table 4** below.

Table 4. ECSA Decay Rate for each FC Configuration.

Number of SC	ECSA Decay Rate [cm^2 Pt / (cm^2 electrode)*(h)]	σ_{rate}
0	-0.11	0.015
1	-0.042	0.0028
3	-0.045	0.0027

However, it is observed the ECSA for both FC configurations reached a similar value around the same time (600-700 h). If the non-hybridized FC decay was to continue, whether it would follow its previous decay rate cannot be concluded from the given results. The power durability comparison results concluded a possible reason for better performance with hybridization could be from less carbon-catalyst structural degradation. ECSA decay could support this idea because

if the catalyst support is degrading at a higher rate, the active surface area would decrease due to agglomeration and corrosion of the carbon-Pt complex.

4.4 Hydrogen Crossover

Using data collected by LSV **(Section 3.4.3)** the average fuel crossover oxidation current was found to be 0.8 mA cm^{-2} for the non-hybridized FC. This is in congruence with expected values for a 1 mm thick *Nafion*® membrane. For the hybridized FC, the average current was very close at about 0.9 mA cm^{-2}. When observing the hydrogen crossover trend, it remains fairly steady for the initial 500 hours of cycling for both FC configurations **(Figure 19)**. Towards the end of the 0SC FC's life (600-700h), the hydrogen crossover spikes nearly 25% which could be the result of membrane thinning and mechanical fatigue if the trend were to continue. The 3SC FC continued to maintain steady crossover until 900h of cycling where it began to experience higher amounts (40-60%) of fuel crossover.

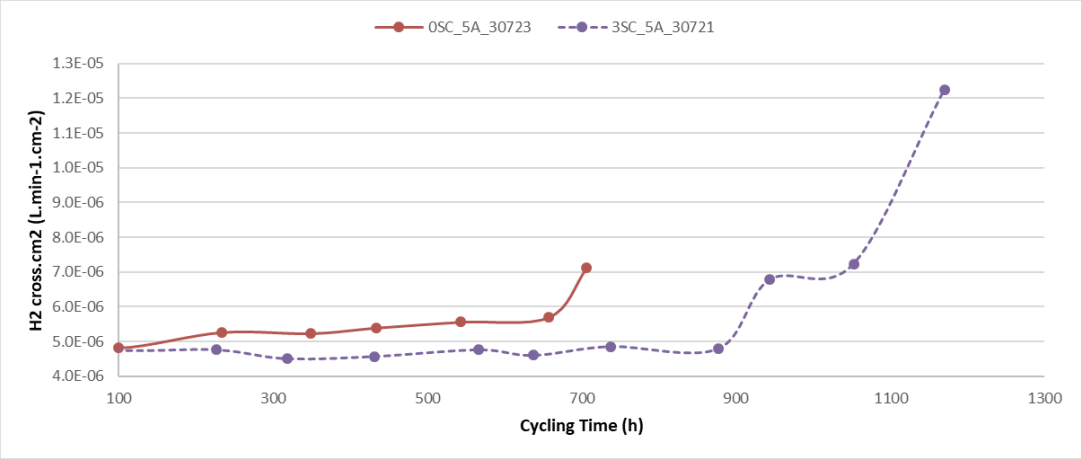

Figure 19. Hydrogen Crossover vs. Hours of Cycling.

This figure portrays the hydrogen crossover profile as the membrane is aged. It is expected the crossover will increase gradually for the majority of the FC lifespan but will then rapidly increase towards the end.

From these data, it is evident the hybridized FC was able to maintain membrane integrity for a longer period of time, as well as still undergo cycling despite the high amounts of fuel crossover towards the later half of its lifespan.

4.5 Fuel Cell Resistance

Ohmic resistance for all runs remained relatively constant and thus was not chosen for analysis, instead, charge transfer resistance (R_c), diffusion resistance (R_{dc}), and their sums were compared. Resistance comparisons were taken at the 20A and 80A characterizations because in the low and high current domain the FC is limited by phenomena shown in R_c and R_{dc} respectively. When hybridized, the sum of resistances (R_c+R_{dc}) was consistently lower throughout the lifetime of the cell. This result coincides with the idea direct hybridization increases the durbaility of the FC through an overall decrease in FC resistances. The percent change for the sum of resistance was

also compared making it easier to observe the rate at which the resistances increased **(Figure 20)**. The non-hybridized FC reached peak resistance 50% faster than the FC with 3SCs. For the 0SC FC's last characterization (700h), it reached a R_c+R_{dc} value ~140% greater than its initial resistance, where the 3SC FC was only at ~15%. For twelve out of the thirteen characterizations, the 3SC FC's resistance change remained significantly below that of the non-hybridized FC.

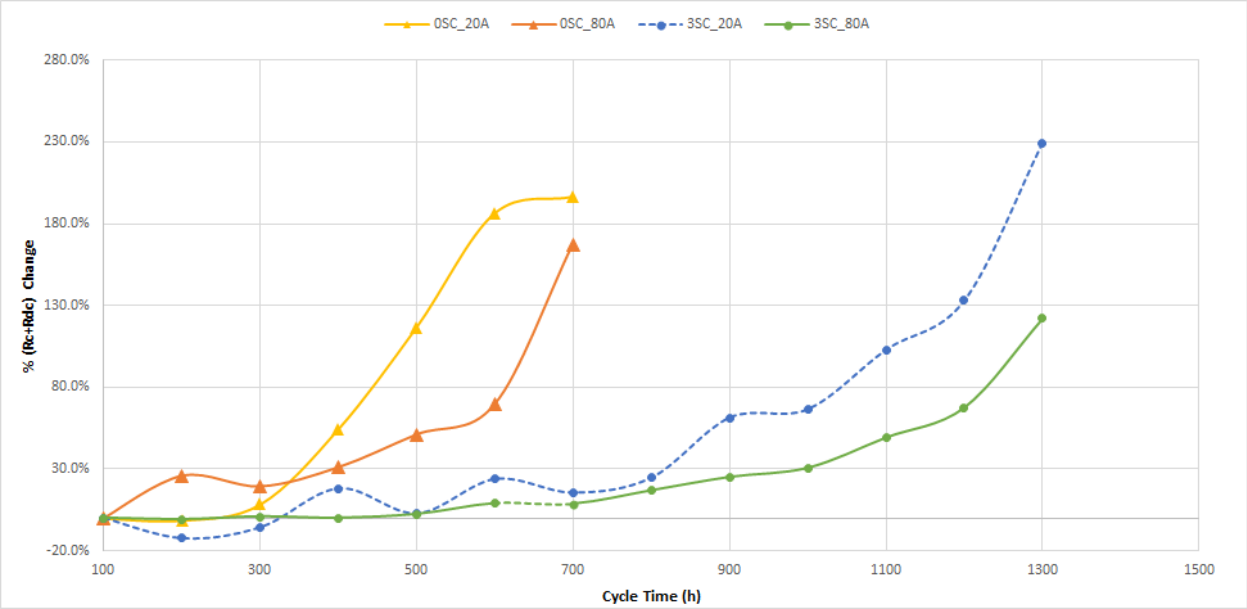

Figure 20. FC Resistance (R_c + R_{dc}) Percent Change Profile vs. Cycle Time (h).
This graph portrays the percent change profile for the diffusion and cathodic sum of resistance for 0SC and 3SC. The change is based of each characterizations difference from the 100h characterization value.

As mentioned previously, at higher amps the FC is in a mass transfer limited domain and can be seen with the R_{dc}. The diffusion resistance was found to decrease for the first 700h of cycling in both hybridized and non-hybridized configurations. To observe this trend, the R_{dc} percentage change was plotted for both 0SC and 3SC FCs **(Figure 21)**. Despite the small initial decrease in R_{dc} for the hybridized FC, the overall trend for both configurations showed an increase in diffusion resistance. The diffusion resistance represents diffusion, absorption and desorption mass transport phenomena. Thus, an increase in R_{dc} is expected in a degrading FC as the membrane is becoming fatigued and mass transport becomes more limited.

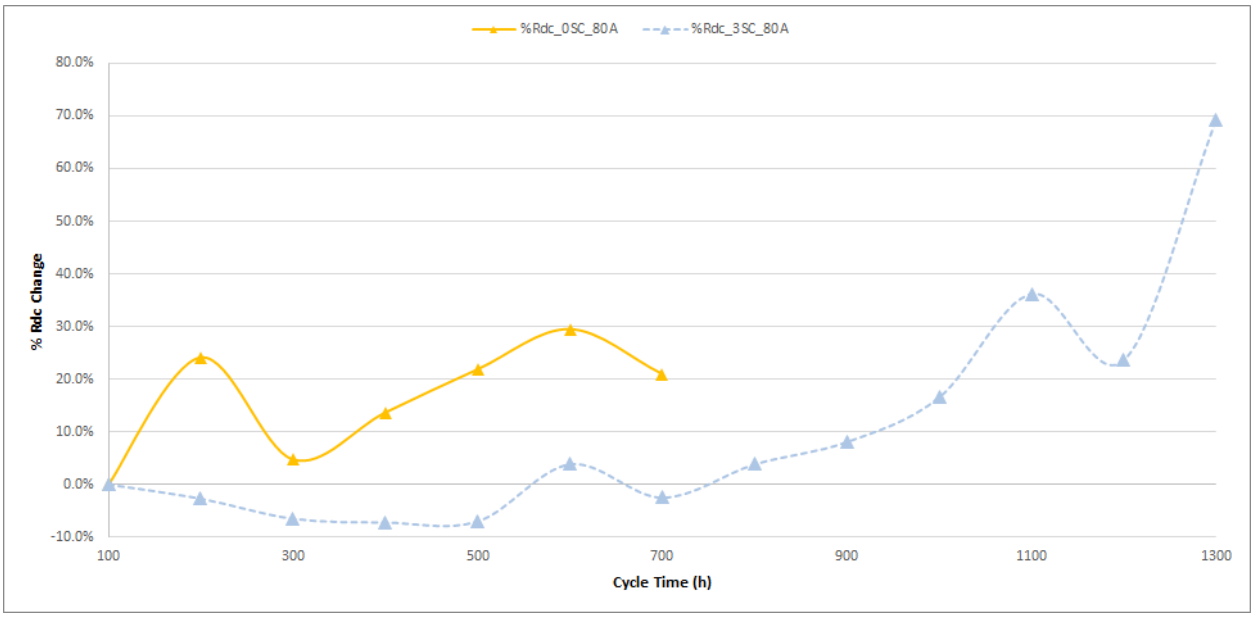

Figure 21. Percent Change of R_{dc} for FC+0SC and FC+3SC.

This finding can be related to the degradation, or reduction, of the carbon-catalyst support in the MEA. It is known from the above results, the non-hybridized FC experienced more rapid power demands during cycling as it worked alone in providing the requested current. Rapid power requests have been found to be a large contributor to degradation of the carbon-catalyst complex [14]. Although the hybridized FC ultimately achieved a higher diffusion resistance, the structural integrity of the membrane was arguably maintained for longer as it had a lower change of resistance for the duration of the the non-hybridized FC's life.

5.0 Conclusion

Based on long-term cycling data and characterization tests comparing the two operational modes (PEMFC directly hybridized and non-hybridized with 1 and 3SC) the results suggest hybridization significantly impacted FC performance by increasing the durability, and ultimately lifespan of the cell. This was justified by an observed increase in cell lifetime from cycling data, a decreased voltage decay, a greater power endurance, as well as a lower rate of increasing resistance, decreased hydrogen crossover, and ECSA decay values. For both FC configurations, the shown increase in resistances points towards membrane degradation, however degradation could also be linked to the Pt catalyst as ECSA also showed a decrease. Objectively, the percent power decay **(Figure 17, Appendix 8.9)** portrays the largest impact of direct hybridization, with a better power endurance and membrane durability.

Another impact of FC hybridization is the FC voltage smoothing effect **(Figure 3)**. When the FC is not hybridized it is responsible for the entire requested load, and when there is a sudden increase or decrease in the power demand the system is shocked. SCs aid the FC by providing the majority of the power in these instances. The results confirm the benefit of directly hybridizing a FC with a supercapacitor, however no comment can be made on the amount of capacitance for optimization. It is our recommendation further testing should be performed in order to both validate results found in this study and to continue to optimize the FC performance. Parameters which still must be considered for optimization include operating conditions, amount of capacitance, current safety limit, inlet fuel stoichiometry, and the quantity of fuel cells operating in series. With this, one could observe the effect on FC durability and degradation, as well as the possibility of decreasing hydrogen consumption for transportation applications. All these parameters should be analyzed with similar (to this study) testing protocols and data processing techniques so trends can be compared.

6.0 Nomenclature

I - Current
A - Ampere
V - Voltage
P - Power
R - Resistance
N - Number of Cell Units
PEMFC - Proton Exchange Membrane Fuel Cell/Polymer Electrolyte Membrane Fuel Cell
FD-DLC - European harmonized Fuel Cell Dynamic Load Cycle
I_{LS} - Current Safety Limit
FC - Fuel Cell
V_{FC} - Fuel Cell Voltage
DC - Direct Current
AC - Alternative Current
PC - Polarization Curve
F - Faraday's Constant
Q - Heat
i - Current Density
j - Imaginary Number
R_c - Charge Transfer Resistance
R_{dc} - Diffusion Resistance
R_{ohm} - Ohmic Resistance

7.0 References

[1]Thounthong, P., Chunkag, V., Sethakul, P., Davat, B., Hinaje, M. *Comparative Study of Fuel-Cell Vehicle Hybridization with Battery or Supercapacitor Storage Device*. IEEE Transactions on Vehicular Technology, Vol. 58, No. 8. October 2009. Retrieved Jan. 11, 2018.

[2]Géradin, K., Raël, S., Bonnet, C., Arora, D., Lapicque, F. *Direct Coupling of PEM Fuel Cell to Supercapacitors for Higher Durability and Better Energy Management*. Laboratory for Reactions and Chemical Engineering. Universite Lorraine. Retrieved. Jan 11, 2018.

[3]Arora, D., Géradin, K., Raël, S., Bonnet, C., Lapicque, F. *Effect of Number of Supercapacitors Directly Hybridized with PEMFC on the Component Contribution and the Performance of the System.* Laboratory for Reactions and Chemical Engineering. Universite Lorraine. Retrieved. Jan 11, 2018.

[4]Arora, D., Géradin, K., Raël, S., Bonnet, C., Lapicque, F. *Impact Study on Safety Limit Current in Direct Hybridization of PEMFC and Supercapacitors for Transport Applications*. Accepted for Publication in Journal of Applied Electrochemistry (2018). Retrieved. Jan 11, 2018.

[5]Orazem, Mark E., Tribollet, Bernard. *Electrochemical Impedance Spectroscopy*. The Electrochemical Society (ECS) Series. Retrieved Jan. 12, 2018.

[6]Dicks, A., Larminie, J. *Fuel Cell Systems Explained 2nd Edition*, Wiley, New York, 2003, ISBN 978-0-470-84857-9

[7]Chaparro, A. M., Martin, A.J., Folgado, M.A., Gallardo, B., Daza, L., *Int. J. Hydrogen Energy* 2009, 34, 4838.

[8]Inaba, M., Kinumoto, T., Kiriake, M., Umebayashi, R., Tasaka, A., Ogumi, Z., *Electrochim. Acta* 2006, 51, 5746.

[9]Moein-Jahromi, M., Kermani, M.J. *Performance Prediction of PEM Fuel Cell Cathode Catalyst Layer Using Agglomerate Model.* International Journal of Hydrogen Energy, Volume 37, Issue 23, 2012, ISSN 0360-3199.

[10]Pilatowsky, I., Romero, R.J., Isaza, C.A., Gamboa, S.A., Sebastian, P.J., Rivera, W. *Cogeneration Fuel Cell-Sorption Air Conditioning Systems.* Thermodynamics of Fuel Cells. 2011, XIV, p. 160.

[11]Joint Research Centre (European Commission). *EU Harmonised Test Protocols for PEMFC MEA Testing in Single Cell Configuration for Automotive Applications*. January 2016, ISBN 978-92-79-54132-2, Retrieved Feb 20, 2018.

[12]Jain, N., Roy, A., Jain, R., Karmakar, N.C. *Polymer Electrolyte Membrane Fuel Cells: Alternative to fossil fuels for power supply to Heavy Earth Moving and Allied Machinery in Mining and Civil Engineering Industry.* December 2013, DOI: 10.13140. Retrieved. Feb. 20, 2018.

[13]The Fuel Cell Store: *Education Research and Fun since 1999.* Polarization Curves (example of a PEMFC polarization curve). Oct. 24, 2017. Retrieved. Feb. 20, 2018.

[14]Tang, H., Qi, Z., Elter, J. F., *PEM Fuel Cell Cathode Carbon Corrosion due to the Formation of Air/Fuel Boundary at the Anode.*

[15]Jung, W. S. *Study on Durability of Pt Supported on Graphitized Carbon Under Simulated Start-up/Shut-Down Conditions for Polymer Electrolyte Membrane Fuel Cells*. May, 31, 2017. Retrieved Feb. 21, 2018.

[16]Lin, R., Cui, X., Shan, J., Técher, L., Xiong, F., Zhang, Q. *Investigating the Effect of Start-up and Shut-down Cycles on the Performance of the Proton Exchange Membrane Fuel Cell by Segmented Cell Technology*. Nov. 16, 2015. Retrieved Feb. 21, 2018.

[17]Lin, R., Xiong, F., Técher, L., Zhang, J.M., Ma, J.X. *Investigation of Dynamic Driving Cycle Effect on Performance Degradation and Micro-structure Change of PEM Fuel Cell.* 2014. Retrieved Feb. 21, 2018.

[18] S. Kim et al. *The Effect of Stoichiometry on Dynamic Behavior of a Proton Exchange Membrane Fuel Cell (PEMFC) During Load Change.* Journal of Power Sources 135. 2004. 110–121. Retrieved Feb. 23, 2018

[19] Wu, J., Yuan, X.Z., Wang, H., Blanco, M., Martin, J.J., Zhang, J., Diagnostic tools in PEM fuel cell research: Part I Electrochemical techniques. Int J Hydrog Energy. 2008 Mar. Retrieved Feb. 26, 2018

8.0 Appendices

Appendix 8.1: Equipment & Materials

- Metrohm Autolab compact entry-level potentiostat/galvanostat GSTAT101
- Cole Parmer peristaltic pump (Masterflex L/S Easy-Load II (Model. 77200-50), with precision tubing by Cole Parmer.
- EireLec Ltd. digital thermostat with multiple thermocouples
- Brooks® MF Smart Series MFC/MFM Flow Meter
- RKC Instrument Inc. Multi-point Digital Controller (Model. MA900/MA901)
- Tektronix AC/DC Current Measurement/Amplifier System (Model. TCPA300)
- Rohde & Schwarz HMP4030/HMP4040 Programmable Three/Four-Channel Power Supply
- LAUDA ECO Silver Immersion thermostat
- Huber high precision thermoregulation Compatible Control
- Telonic Instrument for the Kikusui electronic load

Appendix 8.2: Fuel Cell Construction

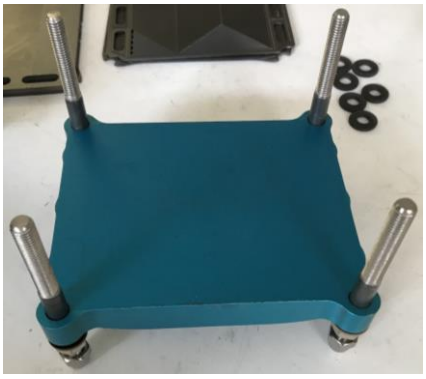

1)

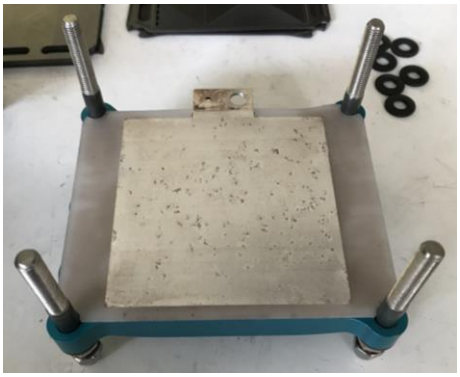

2)

3)

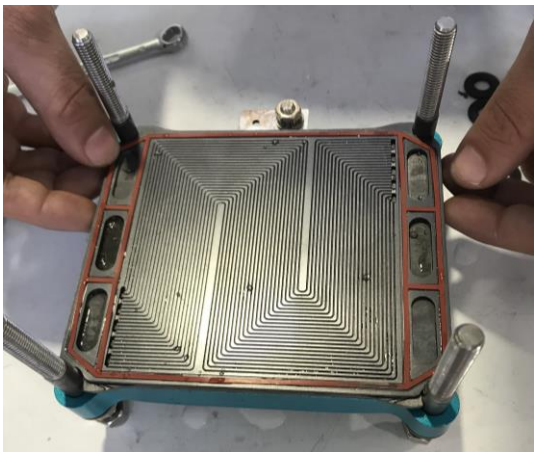

4)

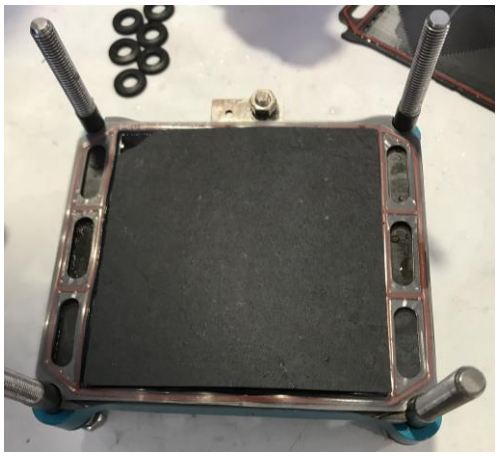

5)

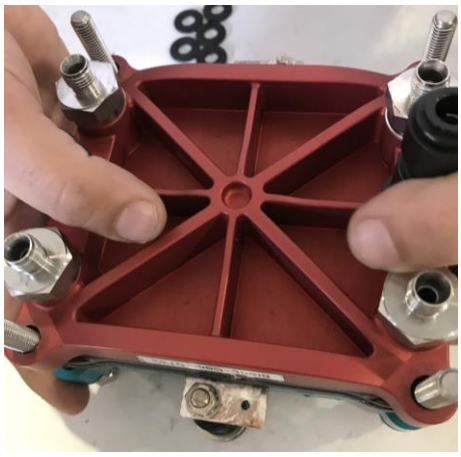

6)

1) Fuel Cell End Plate
2) Bipolar Plates
3) Cooling/Heating Water Plate
4) Gas Plate
5) Gas Diffusion Layer (GDL) + Membrane Electrode Assembly (MEA)

There is a symmetrical configuration on other side of GDL/MEA (i.e. gas plate, cooling/heating water plate, bipolar plate, and then fuel cell end plate to finally form the completed fuel cell stack).

6) Fuel Cell End Plate

Upon tightening (to specified torque) via nuts and bolts, the single cell fuel cell is complete.

Appendix 8.3: Controldesk® User Interface

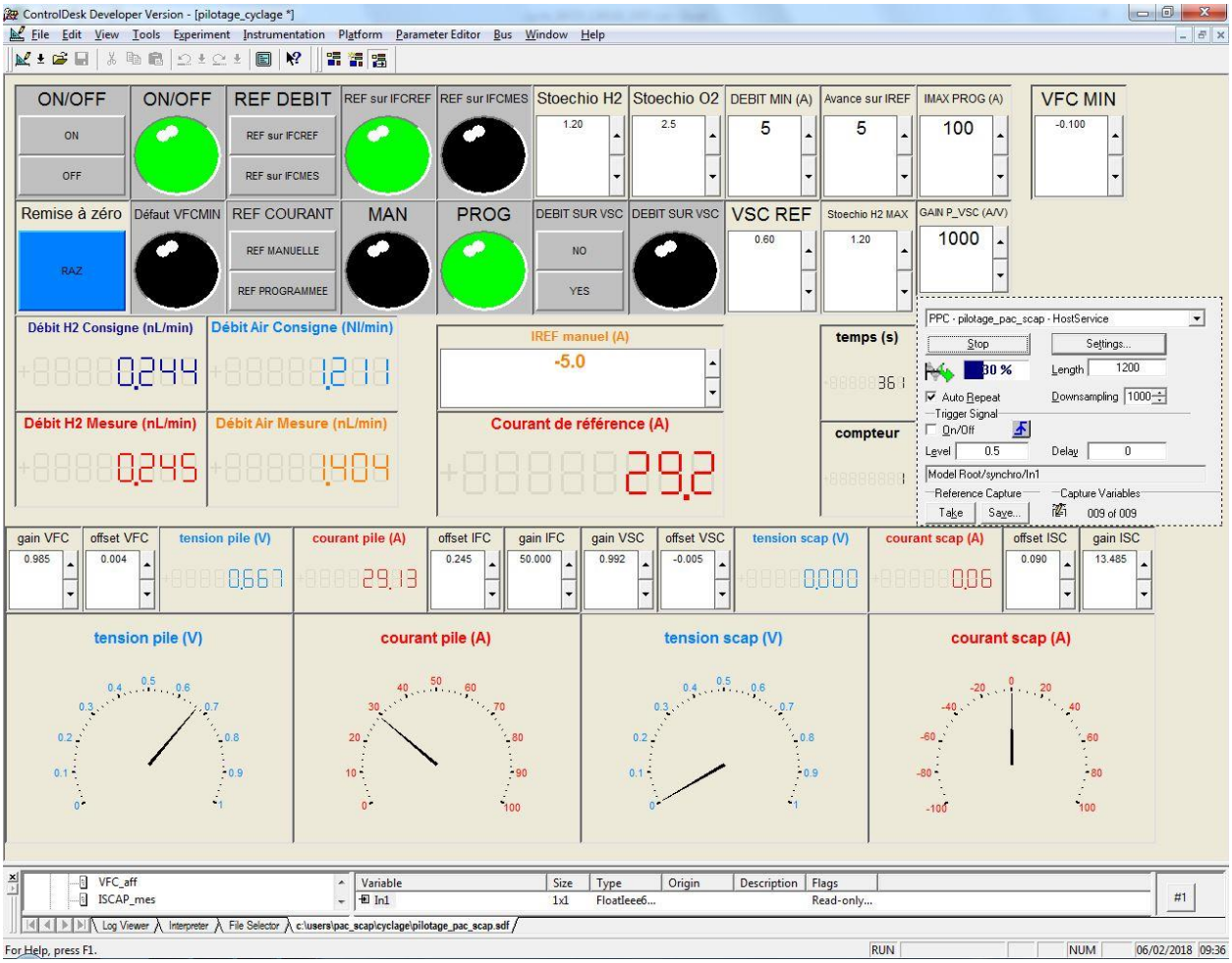

Appendix 8.4: Beginning and End Cycle Comparison for FC+0SC I_{SL} = 0.05A cm^{-2}

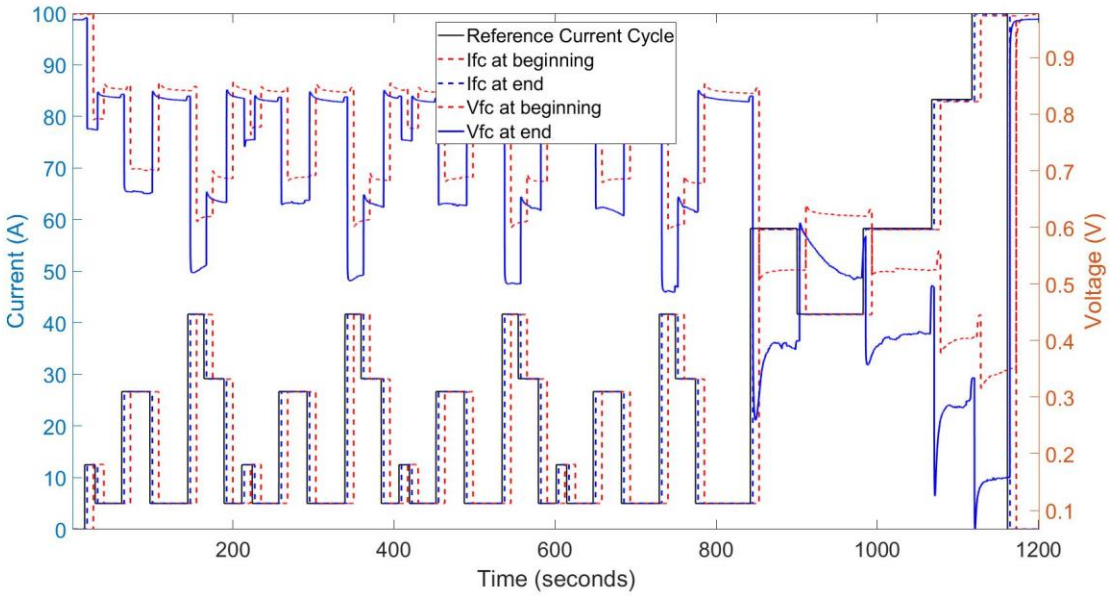

Appendix 8.5: Evolution of Voltage for FC+0SC I_{SL} = 0.05A cm^{-2}

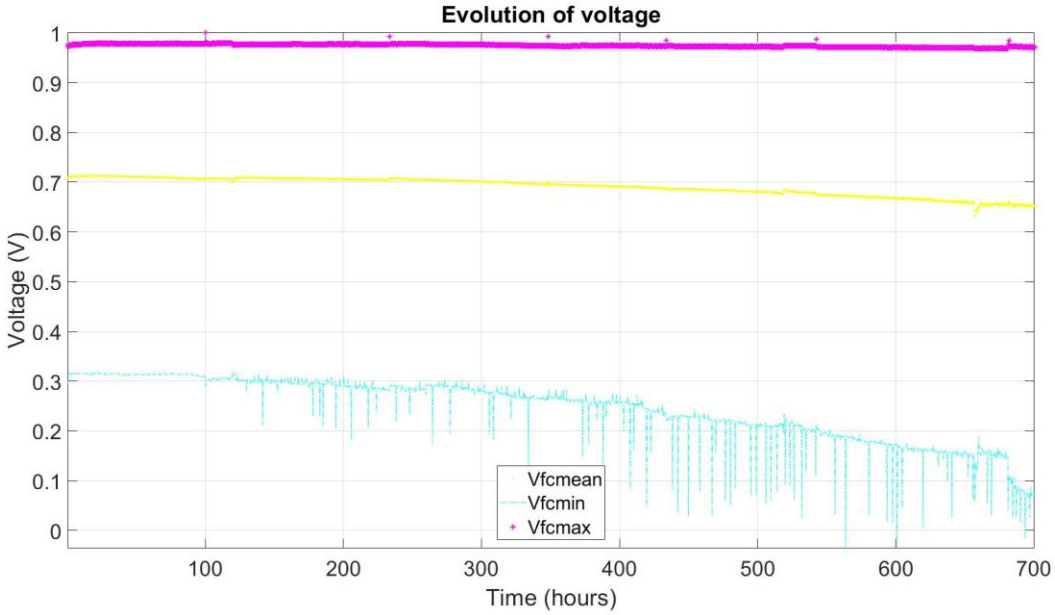

Appendix 8.6: Percent Resistance Evolution of Rdc & Rdc+Rc

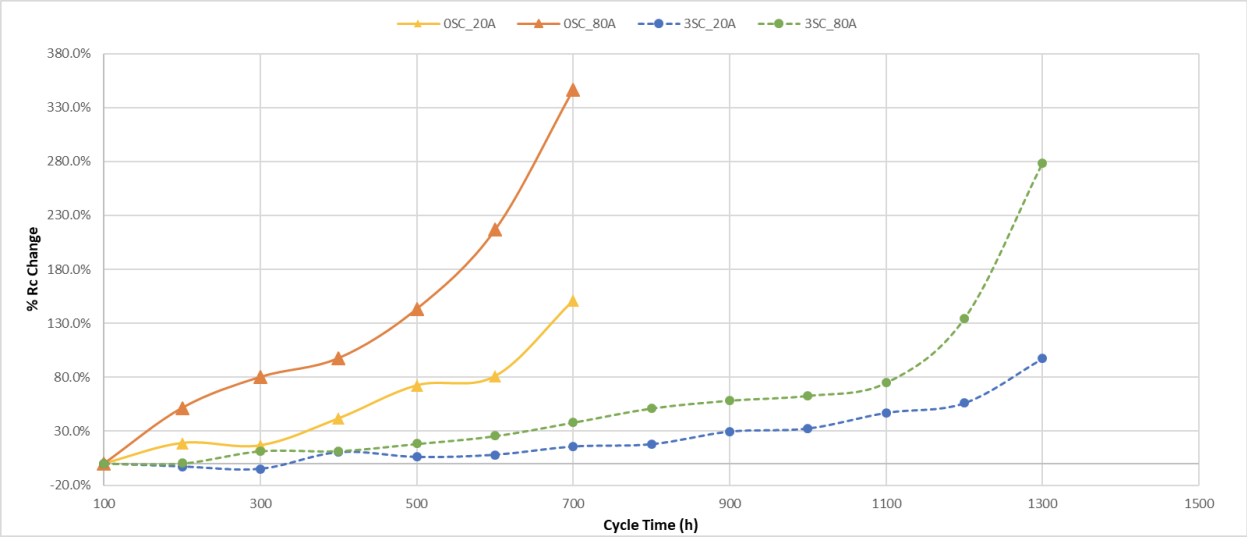

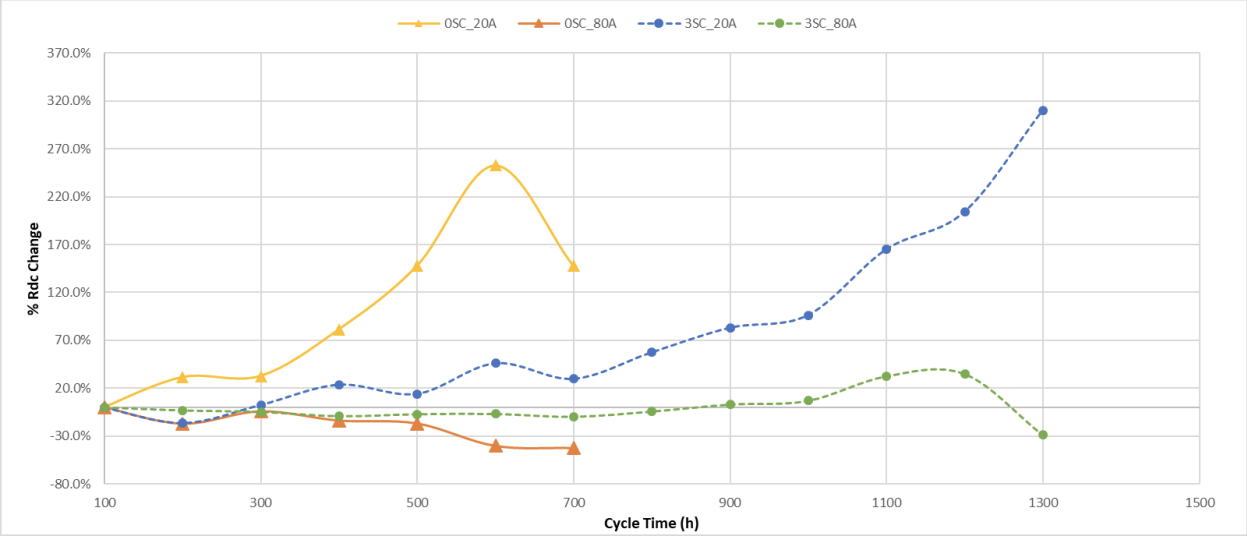

Appendix 8.7: Resistance Evolution of Rdc & Rdc+Rc

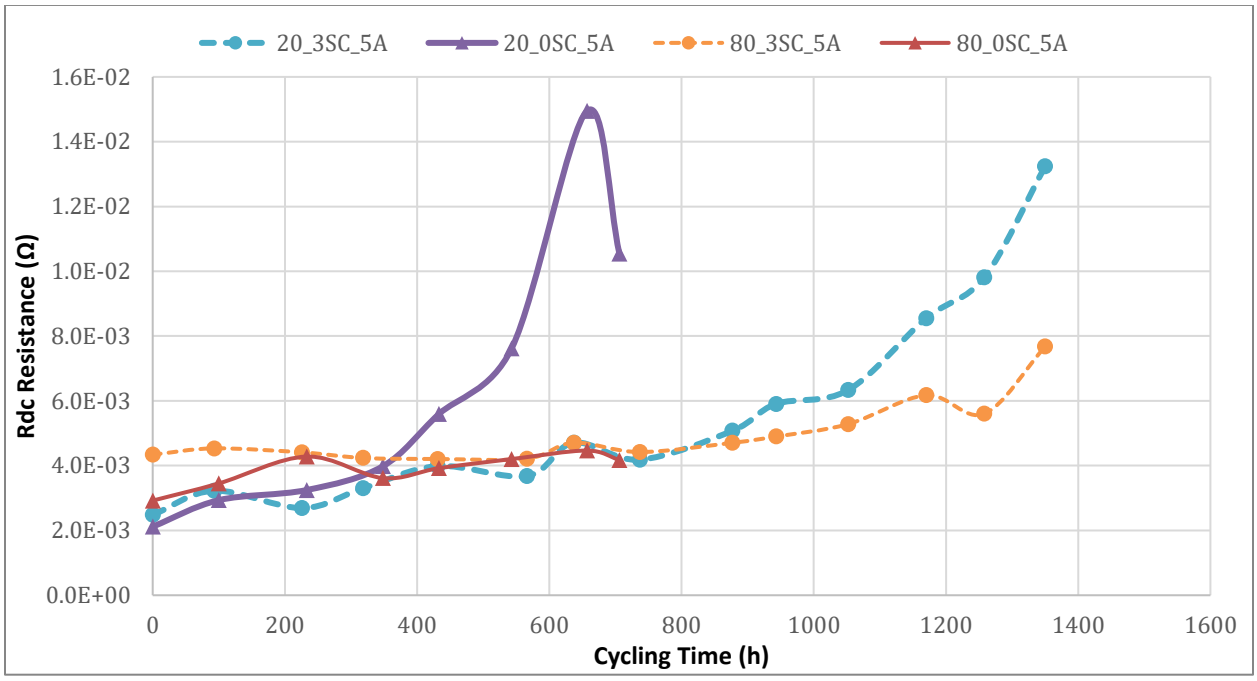

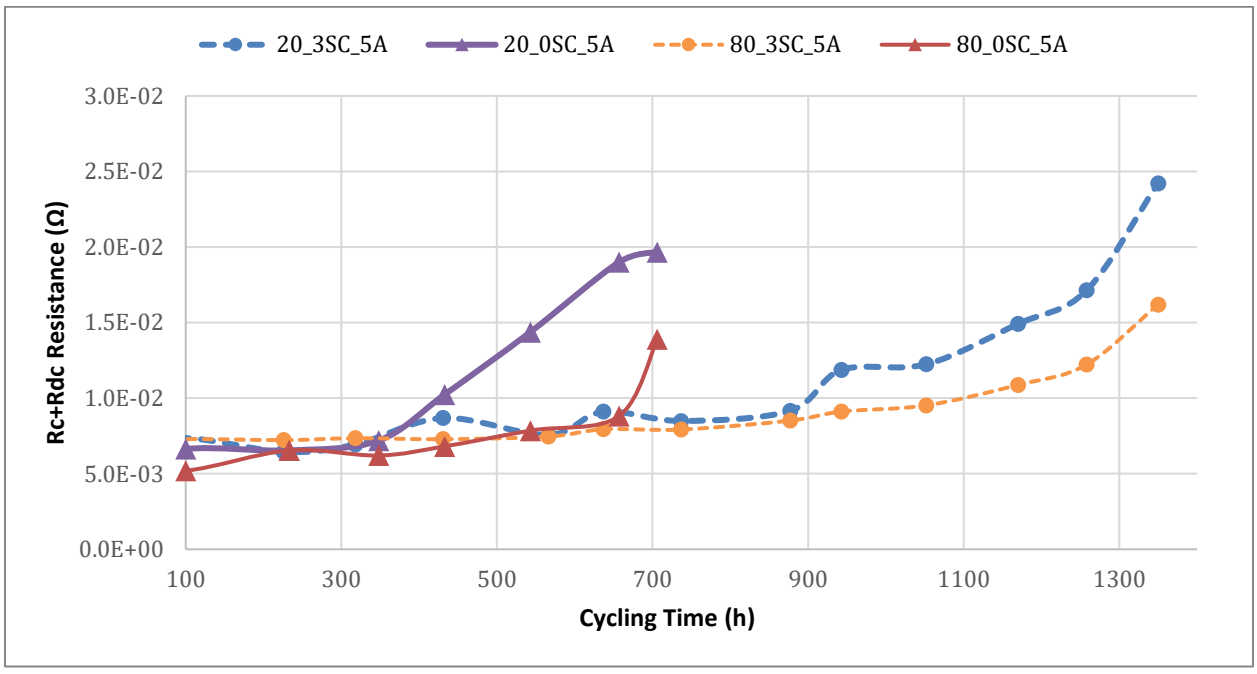

Appendix 8.8: Equivalent Fuel Cell Circuit for EIS Fitting

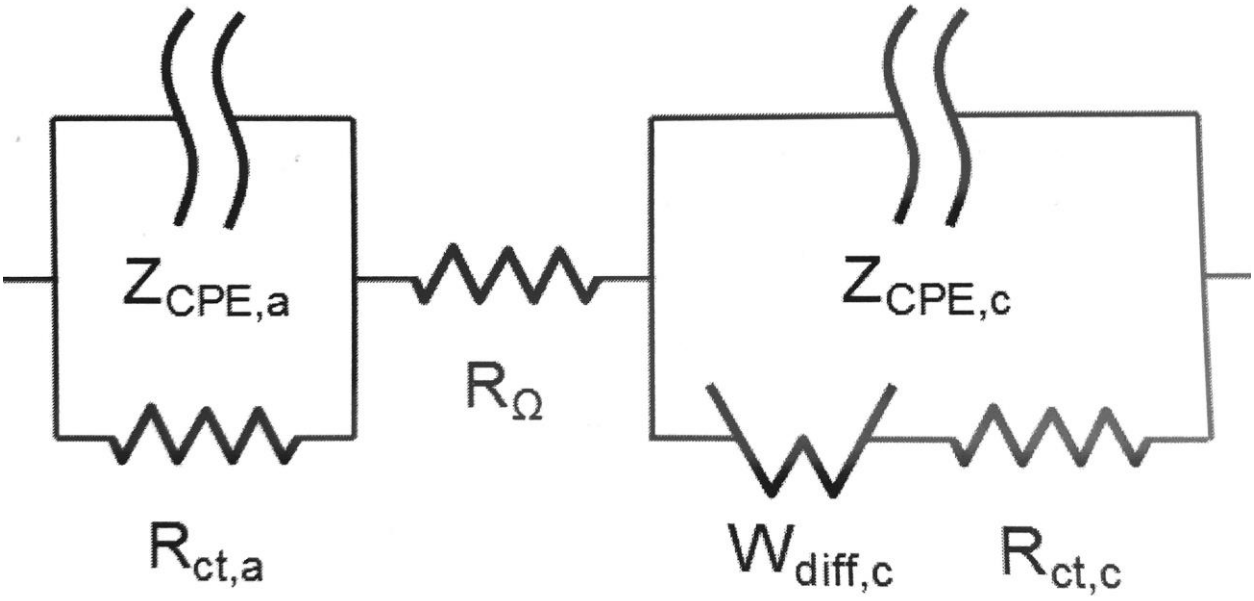

$Z_{CPE,a}$ = impedance constant phase element, anode
Z_{CPEb} = impedance constant phase element, cathode
$R_{ct,a}$ = anodic charge transfer resistance
R_{ohm} = ohmic resistance,
$W_{diff,c}$ = Warburg diffusion resistance
$R_{ct,c}$ = cathodic charge transfer resistance

Appendix 8.9: Evolution of I_{FC}, H_2 consumption

Power yield for FC+0SC at I_{SL} = 0.05A cm^{-2}

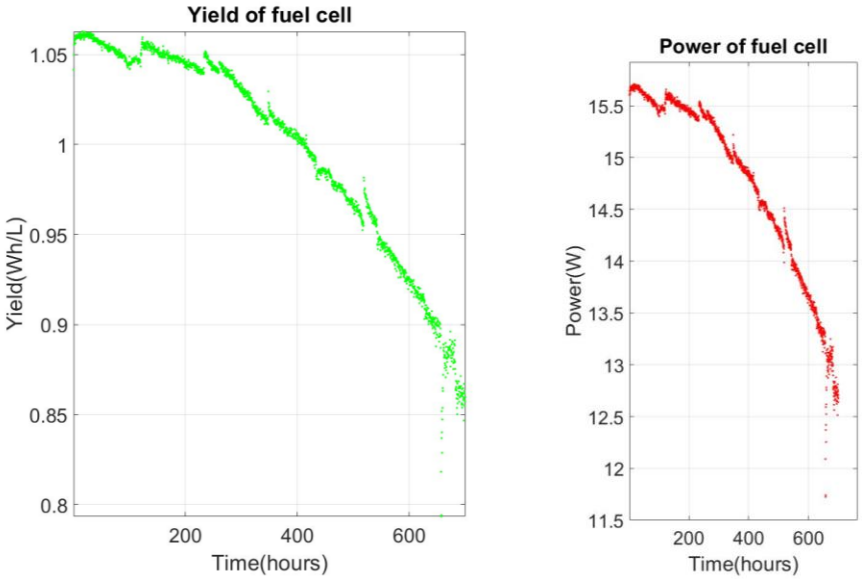

Power yield for FC+3SC at I_{SL} = 0.05A cm-2